UNIVERSITI
MALAYSIA
KELANTAN

The Study of Dispenser on LED Encapsulation using Computational Fluid Dynamics (CFD)

Lam Jun Lok

J20G0747

A report submitted in fulfilment of the requirements for the degree of Bachelor of Applied Science (Material Technology) with Honours

FACULTY OF BIOENGINEERING AND TECHNOLOGY

UMK

2023

DECLARATION

I declare that this thesis entitled "The Study of Dispenser on LED Encapsulation using Computational Fluid Dynamics (CFD)" is the results of my own research except as cited in the references.

Signature : 

Student's Name : LAM JUN LOK

Date : 23/2/2024

Verified by:

Signature : _____

Supervisor's Name : _____

Stamp : _____

Date : _____

ACKNOWLEDGEMENT

Firstly, I wish to express my utmost gratitude to my supervisor, Dr. Muhammad Iqbal Bin Ahmad who bestowed upon me this golden opportunity to carry out this interesting project following the study of 'LED Encapsulation using Computational Fluid Dynamics (CFD)' and the title of 'The Study of Dispenser on LED Encapsulation using Computational Fluid Dynamics (CFD)'. I am really grateful to Dr. Muhammad Iqbal Bin Ahmad as he has guided and helped me with my research with dedication and care, from the submission of my proposal until the completion of my whole project. Hence, I have learnt about so many new and eye-opening information, and I was able to finish my final year project within the allocated time.

In addition, I also give my sincere appreciation to the laboratory assistants, Encik Muhamad Qamal Bin Othman and Ts. Hanisah Izati Binti Adli for their help in assisting me in carrying out my project's experiment.

I am also thankful to University Malaysia Kelantan for the opportunity to pursue my studies. Lastly, I would like to express my deepest gratitude to my beloved parents, Lam Tuck Seong and Koh Poh Geok who have always given me their valuable support. Conclusively, to those who have indirectly contributed to this research, your support means a lot to me.

The Study of Dispenser on LED Encapsulation using Computational Fluid Dynamics (CFD)

ABSTRACT

The purpose of this research study is to observe the effects of dispenser in the process of LED encapsulation using Computational Fluid Dynamics (CFD) and compare the effects of different dispenser parameters on the formation of micro voids in the encapsulation process. This study was aimed to observe a variety of dispenser parameters, which can significantly affect the formation of micro voids in the encapsulation process of LEDs. An LED's performance is heavily impacted by the quality of its packaging. Any formation of micro voids during the encapsulation process of LED packaging can lead to various adverse effects such as the initiation and propagation of cracks. Consequently, this ends in the shortening of the LED's product lifespan as the structural integrity of the packaging is damaged. Thus, this research would utilise ANSYS Fluent software to perform CFD simulation using epoxy resin, an 18G dispensing needle, and an LED5050 chip. By following the materials and measurements made during the physical experimentation setup, the 2D model would be created by using ANSYS Discovery and the analysis of the micro void formation is done using the Multiphase model of ANSYS Fluent CFD simulation. Additionally, the graphical results are interpreted referring to current journal studies.

Keywords: LED Packaging, Encapsulation, Epoxy resin, Computational Fluid Dynamics (CFD), and Micro voids

Kajian Ketinggian Jarum Dispenser pada Enkapsulasi LED menggunakan Computational Fluid Dynamics (CFD)

ABSTRAK

Tujuan kajian penyelidikan ini adalah untuk melihat kesan jarum dispenser dalam proses pengkapsulan LED menggunakan Computational Fluid Dynamics (CFD) dan membandingkan kesan parameter jarum dispenser yang berbeza terhadap pembentukan kekosongan mikro dalam proses enkapsulasi. Kajian ini bertujuan untuk melihat pelbagai parameter jarum dispenser, yang boleh menjejaskan pembentukan kekosongan mikro dalam proses pengkapsulan LED. Prestasi LED sangat dipengaruhi oleh kualiti pembungkusannya. Sebarang pembentukan kekosongan mikro semasa proses enkapsulasi pembungkusan LED boleh membawa kepada pelbagai kesan buruk seperti permulaan dan penyebaran retakan. Akibatnya, ini berakhir dengan memendekkan jangka hayat produk LED kerana integriti struktur pembungkusan rosak. Oleh itu, penyelidikan ini akan menggunakan perisian ANSYS Fluent untuk melakukan simulasi CFD menggunakan resin epoksi, jarum pendispensan 18G dan cip LED5050. Dengan mengikut bahan dan ukuran yang dibuat semasa persediaan eksperimen fizikal, model 2D akan dibuat dengan menggunakan ANSYS Discovery dan analisis pembentukan kekosongan mikro dilakukan menggunakan model Multifasa simulasi ANSYS Fluent CFD. Selain itu, keputusan grafik ditafsirkan merujuk kepada kajian jurnal semasa.

Kata Kunci: Pembungkusan LED, Enkapsulasi, resin epoksi, Computational Fluid Dynamics (CFD), dan lompang Mikro

TABLE OF CONTENT

LIST OF TABLES

LIST OF FIGURES

LIST OF ABBREVIATIONS

18G	Eighteen Gauge
2D	Two Dimensional
3D	Three Dimensional
CFD	Computational Fluid Dynamics
EMC	Epoxy Moulding Compound
LED	Light Emitting Diode
POV	Point of View
RGB	Red, Green, and Blue
RI	Refractive Index
SMD	Surface Mounted Diode
VOF	Volume of Fluid

LIST OF SYMBOLS

%	Percent
m/s	Velocity
mA	Milliampere
mcd	Millicandela
ml	Millilitre
mm	Millimetre
MPa	Megapascal
N	Newton
N/m	Newton per metre
º C	Degree Celsius
Pa	Pascal
s	Seconds
t	Time
V	Voltage
η	Viscosity
ρ	Density
γ	Strain rate
τ	Shear stress

CHAPTER 1

INTRODUCTION

1.1 Background of Study

Light Emitting Diodes (LEDs) have become a popular choice for illumination and display systems. This includes indoor and outdoor applications such as lighting for automotives, electronic displays, traffic signals, and so on. To put into perspective, LEDs account for 55% of the penetration rate of light bulbs in Malaysia in 2021 (Kosai et al., 2021). They are utilised in a wide variety of applications due to their high efficiency, low power consumption, long lifespan, and other benefits. LEDs are highly efficient in converting energy into light, with approximately 80% of the power being converted into light energy and the remaining 20% into heat (Chiang et al., 2016). However, to ensure their reliability and performance, the encapsulation process is critical. The encapsulation of LEDs is a multidisciplinary process that involves the integration of optics, electronics, thermal engineering, and reliability engineering. During encapsulation, the LED chip is embedded in a resin material. In recent years, efforts have been made to further advance in mouldless encapsulation processes such as active lens forming, chemical foaming process, and mouldless dispensing (Rong Zhang et al., 2015). The LED encapsulation process is important because it protects the LED chip from physical damage, moisture, and other environmental factors that can affect its performance and lifespan. The use of epoxy resins for encapsulating LEDs is cost-effective and advantageous due to their high transparency, strong adhesion, excellent mechanical properties, and high refractive index (Gao et al., 2013). The encapsulation material also helps to shape the light emitted by the LED and improves its efficiency by redirecting

stray photons towards the desired direction. The lighting efficiency and LED reliability are greatly affected by the encapsulation material and the encapsulation interface properties (Zhao & Ye, 2013). One critical factor that affects the encapsulation interface is the distance between the epoxy insertion needle and the LED chip.

The performance and reliability of LED devices are highly dependent on the properties of the encapsulant used, which plays a critical role in improving light extraction and protecting the chips from various sources of stress, including heat, light, humidity, and mechanical damage (Bae et al., 2016). Different parameters can be adjusted to enhance the quality of the encapsulation process, which improves the reliability and performance of the LED by reducing the occurrence of micro voids. Therefore, this research aims to investigate the effects different dispenser parameters and the LED chip during LED encapsulation using Computational Fluid Dynamics (CFD) simulation. In this case, CFD is used to simulate the flow of epoxy around the LED chip during encapsulation. The research involves developing a CFD model to simulate the encapsulation process to provide insight into the effects of distance for the needle, which can be used to improve the encapsulation process and enhance the reliability and performance of LEDs by reducing the micro voids that may occur during the process.

Several studies have investigated the effects of other parameters such as the viscosity of the epoxy material, the dispensing rate, and the dispensing pressure on the encapsulation process. However, the effects of the dispenser velocity, offset, height and the LED chip have not been adequately studied. Understanding the effects of these dispenser parameters and the LED chip can help improve the encapsulation process and enhance the reliability and performance of LEDs. In short, the findings of this research have significant implications for the design and manufacture of LED devices, as well as for other encapsulation processes in the electronics industry.

1.2 Problem Statement

The encapsulation process of LEDs is a crucial step that has significant effect on the light extraction efficiency of LED chips (Alim et al., 2021). One detrimental issue is the occurrence of micro voids in the encapsulation. However, the quality of the encapsulation process can be affected by various factors, including the distance between the epoxy insertion needle and the LED chip (Alim et al., 2022). Currently, there is a lack of research on the effects of this parameter on the encapsulation process. Therefore, there is a need to investigate the effects of different dispenser parameters and the LED chip on the encapsulation process using CFD simulation.

1.3 Objectives

1. To validate CFD simulation results via experimental results.
2. To investigate the effects of dispenser parameters and formations of micro void in the LED chip encapsulation process using CFD simulation (ANSYS).

1.4 Scope of Study

This research project focuses on investigating the effects epoxy dispensing needle parameters and the LED chip on the encapsulation process using CFD simulation. The LED is designed in ANSYS simulation software precisely by following current LED designs available in the electronics industry before conducting tests in the ANSYS software. The study involves modelling the dispensing process and analysing the flow of the epoxy material and the formation of micro voids during the encapsulation process. The study is limited to epoxy as the encapsulation material, and the LED package is assumed to have a standard geometry.

1.5 Significance of Study

This research project's significance is in providing a better understanding of the effects the epoxy insertion needle parameters and formation of micro voids in the LED chip during the encapsulation process. Before LEDs can be used in applications, they require packaging and the packaging process for LEDs is crucial as it significantly impacts the final optical performance and reliability of the devices (Luo & Hu, 2014). The findings of this study can help improve the encapsulation process of LEDs, enhancing their reliability and performance. The study can also contribute to the development of new encapsulation techniques and materials that can further improve the quality of LEDs as the packaging process for LED devices not only enhances their reliability and optical characteristics, but it also enables the control and adjustment of their final optical performance (Luo et al., 2016). Overall, this research project can have a significant impact on the LED industry, contributing to the advancement of LED technology.

CHAPTER 2

LITERATURE REVIEW

2.1 Light Emitting Diode 5050 (LED)

LEDs are semiconductor devices that emit light when an electrical current is passed through it. These electronic devices are commonly available in various shapes and sizes for different lighting applications. LED 5050 is a popular type of surface-mounted LED (SMD) that has been widely used in various lighting applications due to its high brightness, efficiency, and versatility.

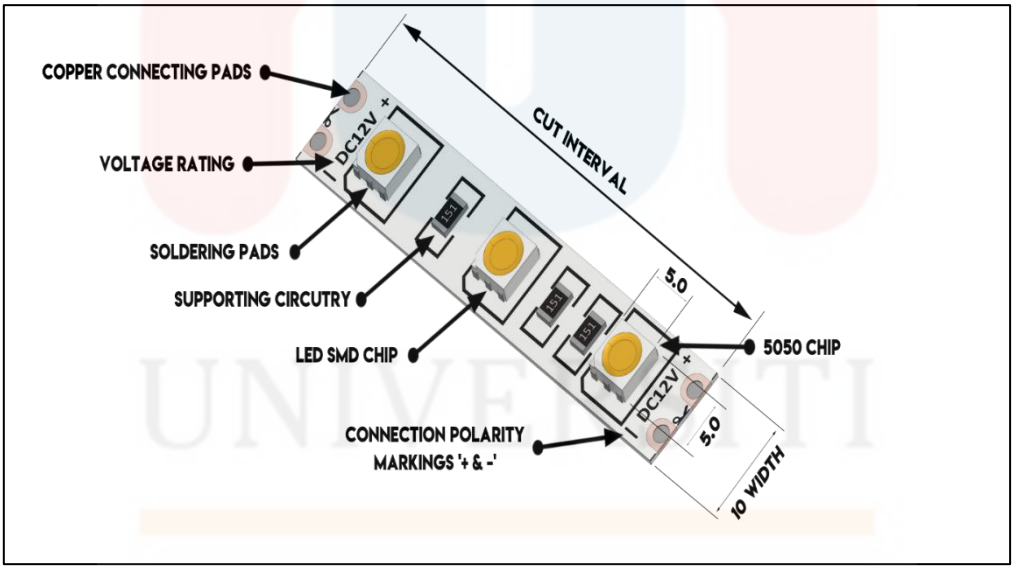

Figure 2.1: Component parts of monochrome LED 5050 strip

(Source: Thaine, 2020)

From Figure 2.1, it is evident that several components play a part in the functionality of a typical monochrome LED 5050 strip. Copper connecting pads are the electrical contact points which allow for the connection of the strip to a power source and control circuitry which enables the illumination of the LED strip. As LED strips are designed to operate at a specific

voltage rating, it is important to depict the appropriate voltage rating on the strip for its correct and safe function. In the figure, 12V is depicted as the voltage rating of the LED strip. Higher voltage rating such as 24V can allow for a longer single length strip design of up to 10 metres instead of 5 metres for 12V voltage rating strips (Thaine, 2020). Soldering pads are areas on the LED strip where additional wires or connectors can be soldered. These pads allow for extension and customisation of the LED strip's wiring configuration with convenience. Supporting circuitry includes components such as resistors or capacitors to regulate the voltage or current flow in the LED strip. Essentially, the supporting circuitry ensures proper operation and protects the LEDs from voltage fluctuations and current surges. The LED SMD Chip are the main component in the LED strip as they are responsible for emitting light and are typically arranged in a desired pattern or spaced along the strip's length as seen in the figure. More specifically, the LED SMD Chips in the figure are 5050-sized chips as labelled. Connection polarity markings are also indicated on the LED strip to ensure correct connection orientation. This is to prevent reverse polarity when connecting to the power supply which can damage the LEDs.

2.1.1 Design

LED 5050 is named after its dimensions, which are 5.0mm × 5.0mm × 0.8mm. It typically consists of three LED chips in a single package, with red, green, and blue (RGB) colours or monochrome single-colour light source.

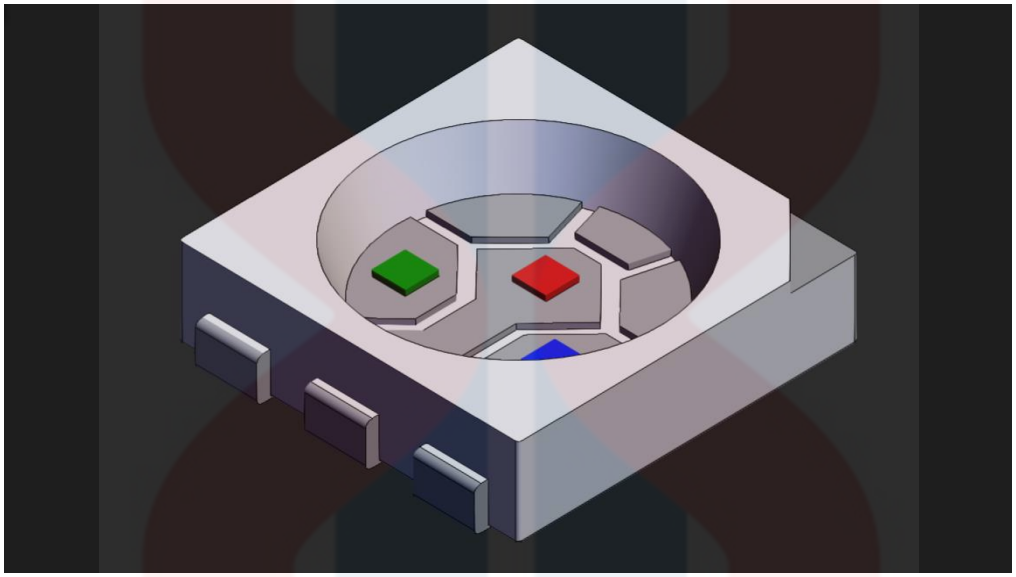

Figure 2.2: Isometric view of a 3D model of a RGB LED 5050

Figure 2.2 depicts an isometric view a 3D model of a RGB LED 5050 design. From the figures, we can observe the standard LED 5050 structure that is present in the design. Key differences LED 5050 designs are the variation in light source colours and the presence of a phosphor layer. The monochrome LED 5050 is available in various colours, including red, green, blue, yellow, amber, and white. Besides that, the monochrome LED 5050 also does not require a phosphor layer. In contrast, the RGB LED 5050 can generate a wider range of colours via colour mixing of the red, green, and blue lights. This means that the RGB variant can accommodate more dynamic and customisable lighting effects by controlling the intensity of each LED chip. Furthermore, the presence of a phosphor layer broadens the colour spectrum by converting a portion of the blue light emitted by the LED chip into green or red light. Additionally, the physical properties of phosphor plays a major role in LED characteristics such as its lifespan and colour-rendering index (Nair, Swart, & Dhoble, 2020).

2.1.2 Electronic Performance

LEDs are known for their high luminous flux and efficiency, which are achieved through unique design and optimized driving conditions. The performance parameters that are often associated with LEDs are power rating, colour, current (mA), voltage (V), and brightness (mcd), (Kuhikar et al., 2020).

Code	Color	Typical Forward Current (mA)	Max Forward Current (mA)	Typical Input Voltage (CV)	Max Input Voltage (CV)	Typical Lm	Max Lm
5055	Red	60mA	75mA	2.0V	2.6V	1800 mcd	850 mcd
5056	Yellow	60mA	75mA	2.2V	2.6V	1800 mcd	900 mcd
5054	Blue	60mA	75mA	3.2V	3.6V	900 mcd	600 mcd
5053	Green	60mA	75mA	3.2V	3.6V	2700 mcd	1800 mcd
5052	White	60mA	75mA	3.2V	3.6V	7700 mcd	3600 mcd
5051	Warm White	60mA	75mA	3.2V	3.6V	7500 mcd	3300 mcd
5050-1	Cold White	60mA	75mA	3.2V	3.6V	8000 mcd	3600 mcd
5057	RGB	60mA	75mA	R 1.8V G 2.8V B 2.8V	2.0V 3.0V 3.2V	500 mcd 1000 mcd 220 mcd	750 mcd 1600 mcd 380 mcd

Table 2.1: Electronic performance of LED 5050 in the industry

(Source: Nationstar LED)

Table 2.1 shows the data sheet for LED 5050 in the industry. From the table, it is evident that the brightness performance of LED 5050 varies depending on the colour of the LED. These electronic properties are key considerations for the outdoor and indoor applications of LEDs where the brightness is crucial.

2.1.3 Applications

LED 5050 is widely used in various lighting applications, including indoor and outdoor lighting, signage, displays. Furthermore, they are also used in other applications such as interior and exterior automotive lighting, backlighting, and signalling (Raypah, Sodipo, Devarajan, & Sulaiman, 2016). It is especially popular in the entertainment and decoration industries, where it is used to create colourful and dynamic lighting effects. LED 5050 is also used in horticultural lighting, where its high efficiency and controllability make it a suitable light source for plant growth. For instance, this recent study uses LED light as a source of light to investigate energy use and nutraceutical properties of indoor-grown lettuce to improve agricultural technologies (Carotti et al., 2021).

2.2 LED Encapsulation

LED encapsulation is a crucial process in LED manufacturing that involves protecting the LED chips and other sensitive components from external factors such as moisture, heat, mechanical stress, and environmental contaminants.

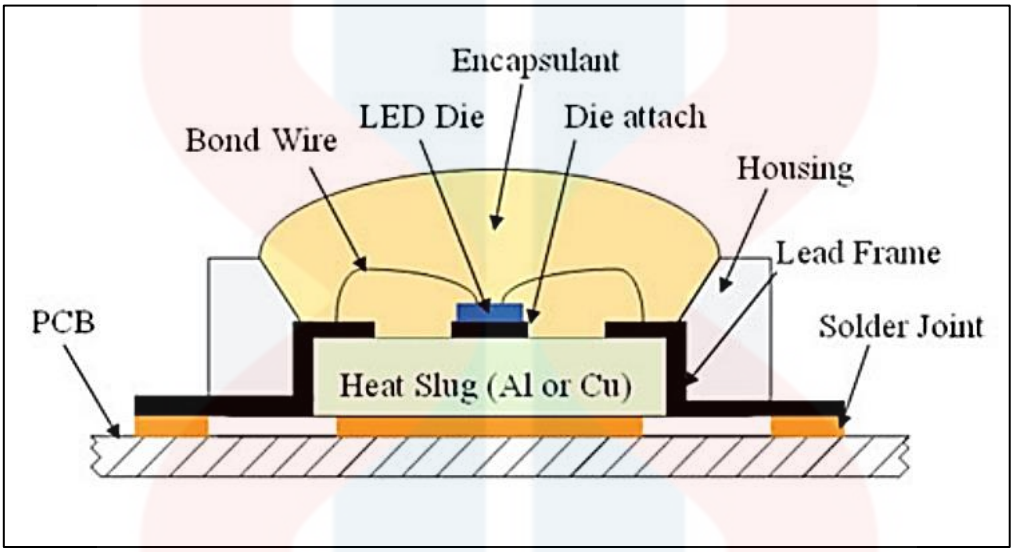

Figure 2.3: LED Package nomenclature

(Source: Pecht et al., 2014)

Figure 2.3 depicts a cross-sectional side view of an LED package, where we can see the components in an LED chip such as bond wire, led die and die attach. More importantly, we observe the encapsulant part of the LED chip. The dome-shaped encapsulant that is positioned over the LED housing is comprised a resin material for the LED package, and it faces multiple failure mechanisms which include carbonization, yellowing, cracking, etc. These failure mechanisms are detrimental to the LED as it causes optical degradation and discoloration of the encapsulant (Pecht et al., 2014).

2.2.1 Technique

There are several techniques employed for LED encapsulation, each with its own advantages and limitations. Some commonly used techniques include active lens forming, chemical foaming process, and mouldless dispensing (Zhang, Lee, & Lo, 2015). Each encapsulation technique has its own considerations, such as curing time, process complexity, cost, and compatibility with different LED chip sizes and package designs. Selecting the appropriate encapsulation technique depends on the specific requirements of the application, including thermal management, optical performance, and reliability. To study the effects of dispenser parameters, the mouldless dispensing technique is used with image-based method to assess the encapsulation (Alim et al., 2022).

2.2.2 Material

Encapsulation materials play a vital role in protecting LED chips and improving their performance. In the field of semiconductor lighting utilizing LEDs, there is a pressing need for encapsulation materials that possess desirable characteristics. These characteristics include exceptional light transmission, a high refractive index (RI), impressive mechanical properties, efficient thermal conductivity, and strong resistance to aging (Shen & Feng, 2023). In modern electronic packaging technology, the majority of encapsulant materials are polymeric materials as they can provide an efficient pathway for heat transfer (Lin, Mcnamara, Liu, Moon, & Wong, 2014). Epoxy resin is commonly used due to its cost-effectiveness, transparency, and good adhesion properties. More notably, epoxy resin is often used in electronics and electrical fields due to their commendable mechanical properties, thermal stability, and especially electrical insulation and chemical resistance (Ruan, Zhong, Shi, Dang, & Gu, 2021). Furthermore, extensive research is still ongoing to improve on epoxy resin as an encapsulation material for packaging applications. For instance, a study recently investigated on the thermal conductivity

of silver-epoxy nanocomposites to be used for electronic packaging (Sun, Li, Yu, Kathaperumal, & Wong, 2022) Additionally, epoxy is also used as an encapsulant in a recent study that also simulated Epoxy Moulding Compound (EMC) in ANSYS software to study LED wire bonding (Roslan et al., 2020).

2.2.3 Micro voids

Micro voids are small air-filled voids or bubbles that can form within the encapsulation material during the LED encapsulation process. Micro voids can occur during the LED encapsulation process due to the presence of moisture or volatile compounds in the encapsulation material, incomplete degassing of the material, inadequate vacuum or pressure conditions, and improper curing parameters. Gap height is one of the dispensing methods which can affect the formation of micro voids in the encapsulation process (Abas et al., 2018). The presence of micro voids in LED encapsulation can have several adverse effects. Firstly, micro voids can scatter or trap light within the encapsulation material, leading to reduced light extraction efficiency and lower luminous intensity of the LED device. This can result in decreased brightness and compromised overall optical performance. Secondly, micro voids can act as stress concentration points, causing mechanical weakness within the encapsulation material. They can lead to the initiation and propagation of cracks or delamination, compromising the structural integrity and long-term reliability of the LED device.

2.2.4 Applications

LED encapsulation has a significant impact on the performance and reliability of LED devices in various applications. LED lighting, including general illumination, architectural lighting, and automotive lighting, relies on effective encapsulation to ensure long-term performance and durability. LED displays and signage require encapsulation that enhances optical properties and protection against external factors. For instance, according to a recent study encapsulation technology is also crucial to protect organic LEDs, organic and perovskite solar cells (Lu et al., 2021).

2.3 Analyses

Computer-aided simulations have become increasingly important in the analysis and optimization of LED designs as these simulations can better solve complex systems in comparison to traditional human trial and error methods (Janai, Woon, & Chan, 2018). Besides that, costs can be driven down through reduction of material use by using computer-aided simulations. With that said, various types of analyses can be performed using computer-aided simulations on LED encapsulation to study its behaviour and performance.

2.3.1 Thermal Analysis

Thermal analysis plays a critical role in LED encapsulation as it helps assess the heat dissipation capabilities and temperature distribution within the LED package. CFD simulations enable the prediction of temperature profiles, hotspot identification, and assessment of thermal management strategies. By incorporating parameters such as thermal conductivity of materials, heat generation within the LED chips, and convective heat transfer, thermal analysis through CFD simulations aids in optimizing the encapsulation design for efficient heat dissipation, reducing thermal stress on the LED chips, and enhancing the overall reliability and performance of the LED device. For example, ANSYS can be used to do a thermal analysis to study the junction temperature (º C) of the LED (Vairavan, Sauli, Retnasamy, et al., 2013).

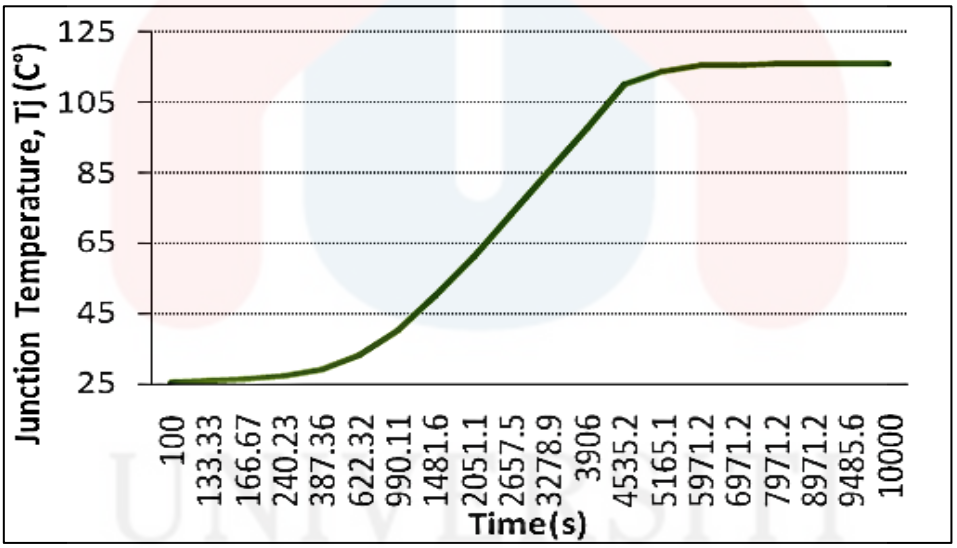

Figure 2.4: Example of ANSYS junction temperature graph

(Source: Vairavan, Sauli, Retnasamy, et al., 2013)

2.3.2 Structural Analysis

Structural analysis using CFD simulations allows for the evaluation of the mechanical integrity and reliability of the LED encapsulation design. By simulating the stress and deformation of the encapsulation materials and package under different operating conditions, structural analysis helps identify potential areas of failure and optimize the design to enhance mechanical robustness. Factors such as material properties, package geometry, and assembly techniques can be studied through CFD simulations to ensure the encapsulation can withstand external mechanical forces and maintain its integrity over the lifetime of the LED device. For instance, the junction temperature obtained from thermal analysis can be used to do a Von Mises stress (MPa) analysis of a 3D model of an LED chip to determine the yield of the LED (Vairavan, Sauli, & Retnasamy, 2013).

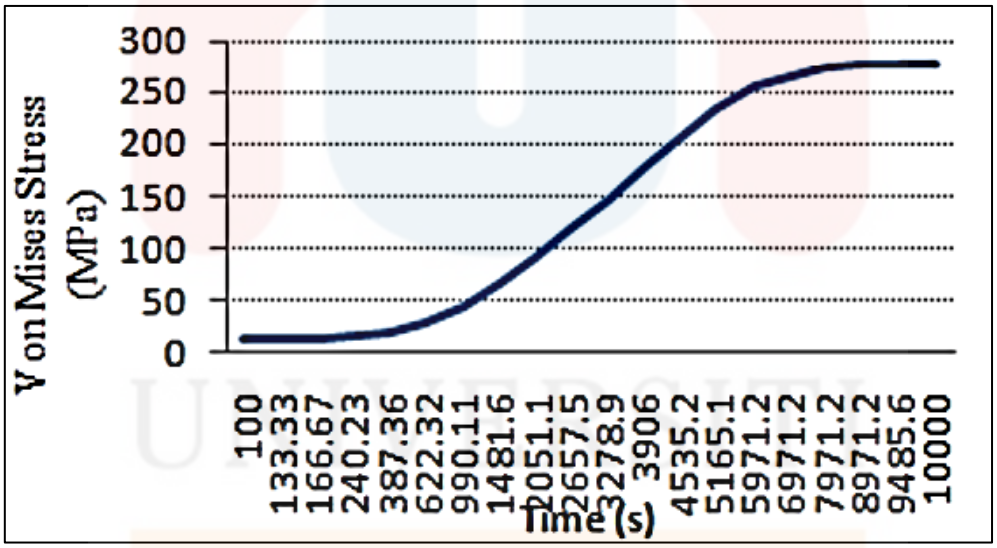

Figure 2.5: Example of Von Mises Stress graph

(Source: Vairavan et al., 2013)

2.3.3 Optical Analysis

Optical analysis using CFD simulations allows for the evaluation LED encapsulation's effect on the LED optical performance. By considering parameters such as refractive index, light scattering, and reflection, CFD simulations can predict light distribution, intensity, and efficiency within the encapsulation structure. This aids in optimizing the encapsulation design for improved light extraction and distribution, minimizing optical losses, and achieving desired lighting effects. Optical analysis using CFD simulations enables researchers and engineers to study and optimize parameters such as encapsulation materials, package design, and surface textures to enhance the overall optical performance and efficiency of LED devices. For example, Zemax OpticStudio software can be used to conduct optical simulation to study the optical performance of LED (Tavakolibasti et al., 2022).

CHAPTER 3

MATERIALS AND METHODS

3.1 Materials

The materials used for researching this encapsulation project are LED 5050 chips, epoxy resin, and dispensing needle. These materials collectively contribute to the encapsulation process of the LED and play a vital role in achieving the desired optical performance, mechanical robustness, and reliability of the encapsulated LED devices. Each of the chosen materials are crucial to enable the investigation of the encapsulation techniques, study of the encapsulation process parameters, and evaluation of the encapsulated LED's performance. By studying the interaction between the materials and refining the encapsulation process, we can gain valuable insights into improving the reliability, efficiency, and longevity of LED devices.

3.1.1 LED 5050 Chip

LED 5050 chip is the type of LED chosen to be used in the experimental and simulation setup for the purposes of this study. More specifically, the monochromatic LED 5050 chip is used as they have a much simpler design. The LED chips are chosen specifically for their characteristics, including their small size (5.0mm × 5.0mm × 0.8mm), high brightness, and ability to emit monochromatic light. They are widely used in various applications due to their versatility and efficiency. Essentially, these LED chips provide the foundation for this study of the encapsulation process and evaluating the performance of the encapsulation materials.

3.1.2 Dispensing Needle

A dispensing needle is used as a tool to dispense the epoxy resin during the encapsulation process. More specifically, a 18G needle is used in the manual dispensing process to control the flow and deposition of the epoxy resin onto the LED 5050 chip. The dispensing needle is attached to a 10ml syringe to allow for a precise application of the resin during the experimental setup. The dimensions of the 18G needle are followed accordingly during the simulation setup. Essentially, the selection of an appropriate dispensing needle ensures accurate and controlled dispensing during the encapsulation process.

3.1.3 Epoxy resin

Epoxy resin is the primary encapsulation material used in this research project. Epoxy resins are a type of polymer that can be characterised by the Epoxide functional group in the polymer molecule.

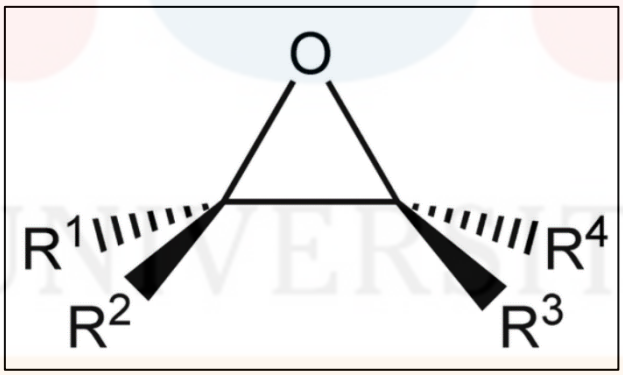

Figure 3.1: Epoxide functional group

Epoxy resin is a thermosetting polymer that offers excellent adhesion, mechanical strength, and protection for the LED 5050 chips. Epoxy resin provides a transparent and protective encapsulation layer, enhancing the durability, reliability, and light transmission efficiency of the LED device. Epoxy resin offers effective protection for the LED 5050 chips against environmental factors such as moisture, dust, and mechanical stress.

3.2 Methods

The study consists of two essential setups which are experimental and simulation setups. The experimental setup requires the use of apparatus such as retort stand, and pump with pressure gauge to conduct a physical LED chip encapsulation with epoxy resin in a laboratory setting. In contrast, ANSYS Discovery software is utilized to create a LED 5050 model during the simulation phase of the project. In the simulation setup, certain components of the LED model are removed, leaving only the essential parts. Essentially this means only the encapsulation site and dispensing needle tip is simulated. The setup includes discussions on the boundary conditions. The simulation results are obtained by repeating the simulation with different dispenser parameters such as height, velocity, and offset. Epoxy dispensing experiment is done to validate the simulation results with the experimental results. By validating the results, the effects of dispenser parameters and the formation of micro voids during the encapsulation process is studied.

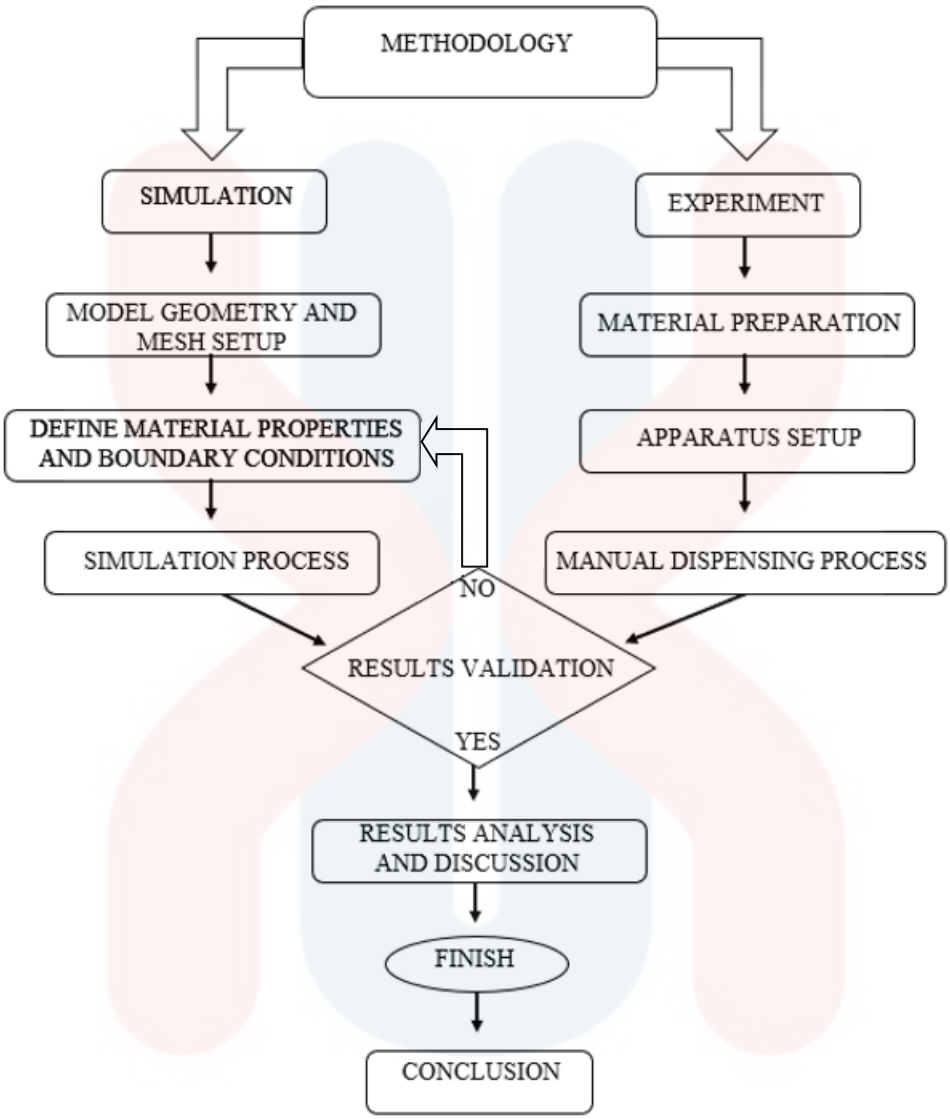

Figure 3.2: Research Flow Chart

Figure 3.2 depicts the research flow chart of the simulation and experiment process. In short, this is the procedure done to validate results and simulate the LED encapsulation process using different dispenser parameters.

3.2.1 Experimental Setup

The aim of the LED encapsulation experiment is to validate the results obtained from the simulation with the actual results. For the experiment, the material and apparatus needed are a camera with tripod, retort stand with clamp, diaphragm pump, 10 ml syringe, a 18G needle with tip of 0.8mm in diameter, a LED 5050 chip, and epoxy resin.

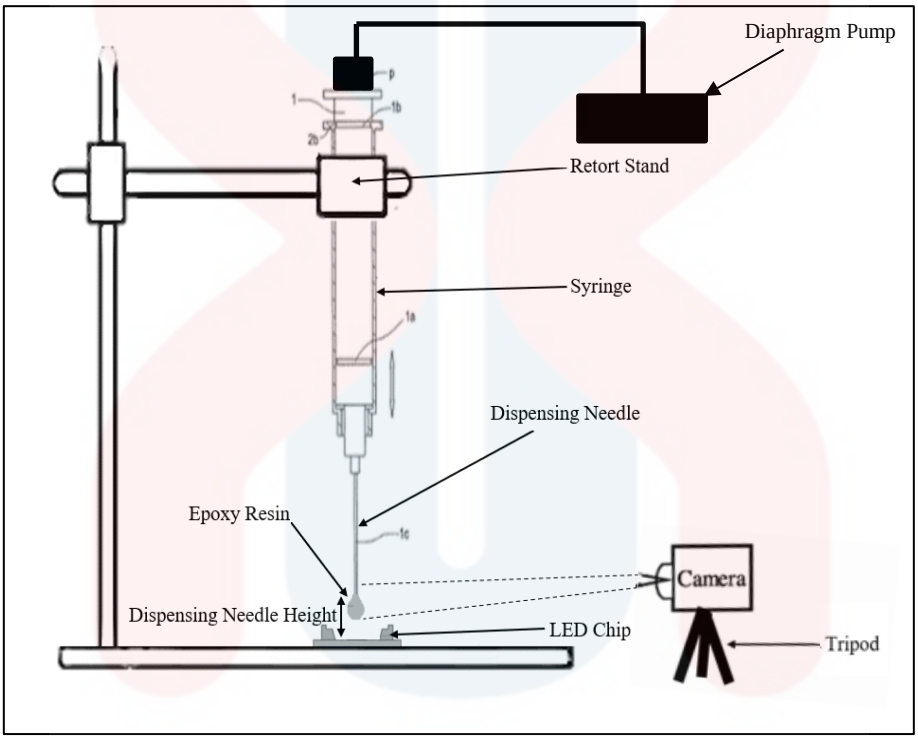

Figure 3.3: Schematic of experiment setup

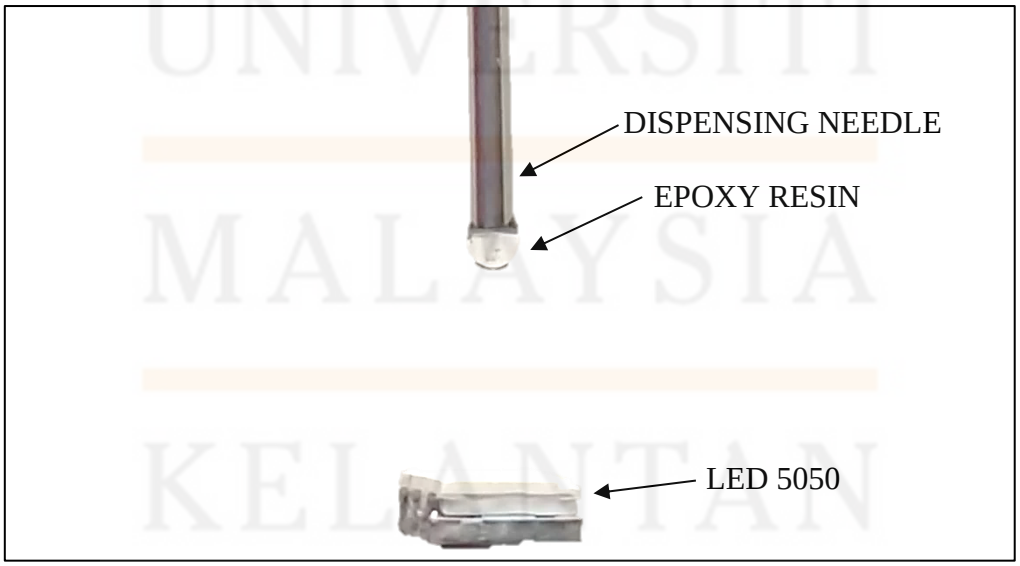

Figure 3.4: Camera POV of experiment setup

Figures 3.3 & 3.4 depict the schematic and depicts the POV of the camera setup for the experiment which aims to capture the encapsulation process. The experiment is conducted with a few parameters assumed to be constant such as airflow, temperature, and pressure. Photos of the experiment are taken as the experiment is conducted to be analysed and included in the results. The analysed result is used to validate the simulation results obtained from the ANSYS software.

3.2.2 Experimental Procedure

First, the LED 5050 chip's dimensions are measured using callipers. The LED is then placed on a clean flat surface with contrast on the retort stand base to have stability and a good view of the encapsulation process. Next, a small amount of epoxy resin is measured, mixed, and put into the 10ml syringe. Then, a diaphragm pump is attached firmly onto the 10ml syringe. After that, a distance of 10mm is measured between the LED chip and the needle tip using the callipers. The pump is then used to inject the epoxy resin onto the LED surface while the pressure gauge is recorded and tabulated. The mould cavity of the LED 5050 substrate allows the fluid to form a hemisphere shape. The fluid dispensing process is recorded using a camera. The experiment is repeated to obtain an average pressure reading and the results are analysed and included in the results to be studied. The obtained experiment results are then studied with the results obtained from the CFD simulation from ANSYS software.

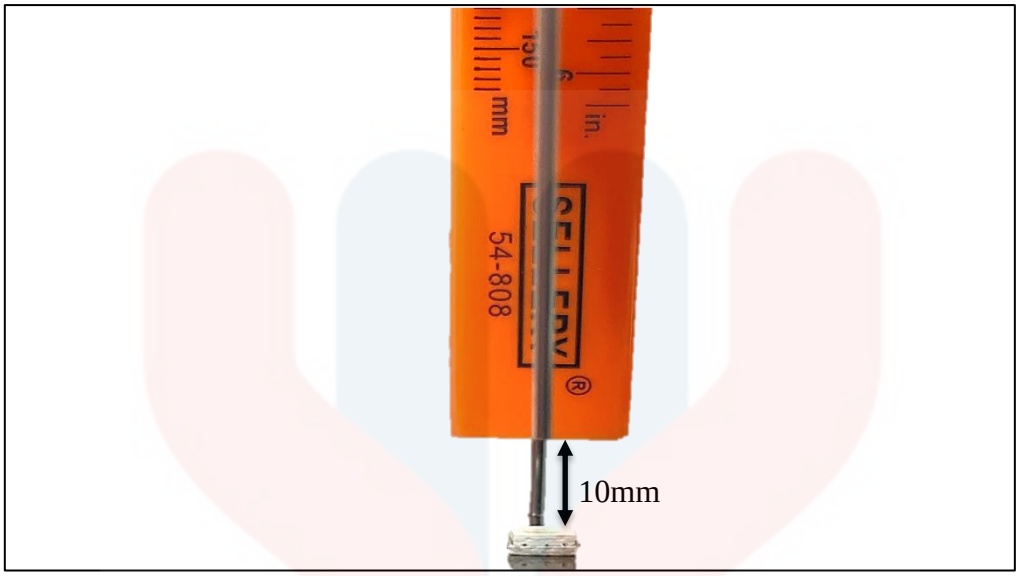

Figure 3.5: Measurement of needle height using callipers

3.2.3 Governing Equation

During the simulation modelling, the Volume of Fluid (VOF) method is used to simulate the encapsulation process of the LED in the simulation software (ANSYS Fluent). More specifically, it is used to calculate the flow of epoxy resin that is dispensed onto the LED 5050 chip.

Epoxy resin fluid flow during the simulation is shown by using two-dimensional incompressible flow transport equations which are continuity (conservation of mass), Navier-Stokes, Newtonian fluids, and conversation of energy equations. The equations are written as follows:

Continuity (conservation of mass) equation:

$$\frac{\partial u}{\partial x} + \frac{\partial v}{\partial y} = 0 \tag{1}$$

where u and v are velocities of the fluid that flow in x and y axis respectively.

The Navier-Stokes equation for x-direction:

$$\frac{\partial u}{\partial t} + u\frac{\partial u}{\partial x} + v\frac{\partial u}{\partial y} = -\frac{1}{\rho}\frac{\partial P}{\partial x} + \left[\frac{\partial}{\partial x}\left(\eta\frac{\partial u}{\partial x}\right) + \frac{\partial}{\partial y}\left(\eta\frac{\partial u}{\partial y}\right)\right] + g_x \tag{2}$$

The Navier-Stokes equation for y-direction:

$$\frac{\partial v}{\partial t} + u\frac{\partial v}{\partial x} + v\frac{\partial v}{\partial y} = -\frac{1}{\rho}\frac{\partial P}{\partial y} + \left[\frac{\partial}{\partial x}\left(\eta\frac{\partial v}{\partial x}\right) + \frac{\partial}{\partial}\left(\eta\frac{\partial v}{\partial y}\right)\right] + g_y \tag{3}$$

where

ρ = density

t = time

u = velocity vector in x-direction

η = viscosity

v = velocity vector in y-direction

gx and gy = gravity in x and y-axis

P = static pressure

The epoxy viscosity is assumed to be constant at high temperature. So, the Newtonian fluid equation:

$$\eta = \frac{\tau}{\gamma} \tag{4}$$

where

τ = shear stress γ = strain rate.

The capacity of the VOF model is to determine and clarify the distribution of the liquid phase by assigning a scalar F in each cell in the computational network. In the model, F indicates the fraction of the cell's volume occupied by the epoxy material. Hence, F takes the value of 1 in the cells containing only the resin, the value 0 in cells void of resin, and the value between 0 and 1 is in the "interface' cells referred to as the epoxy flow front.

The epoxy flow front is represented by the following transport equation:

$$\frac{\partial F}{\partial t} = \frac{\partial F}{\partial t} + u\frac{\partial F}{\partial t} + v\frac{\partial F}{\partial t} - \left\{\frac{\partial^2 F}{\partial x^2} + \frac{\partial^2 F}{\partial y^2}\right\} = 0 \tag{5}$$

The epoxy resin's surface tension is represented by the following equation:

$$\gamma = \frac{F}{L} \tag{6}$$

where

γ = surface tension

F = force acting perpendicular to the surface

L = length along which the force acts

3.2.4 Simulation Setup

In the modelling of the LED 5050 chip, the complete 2D geometry is drawn by using ANSYS Discovery software. The geometry is drawn according to the dimension obtained from the measurement of LED during the experimental setup.

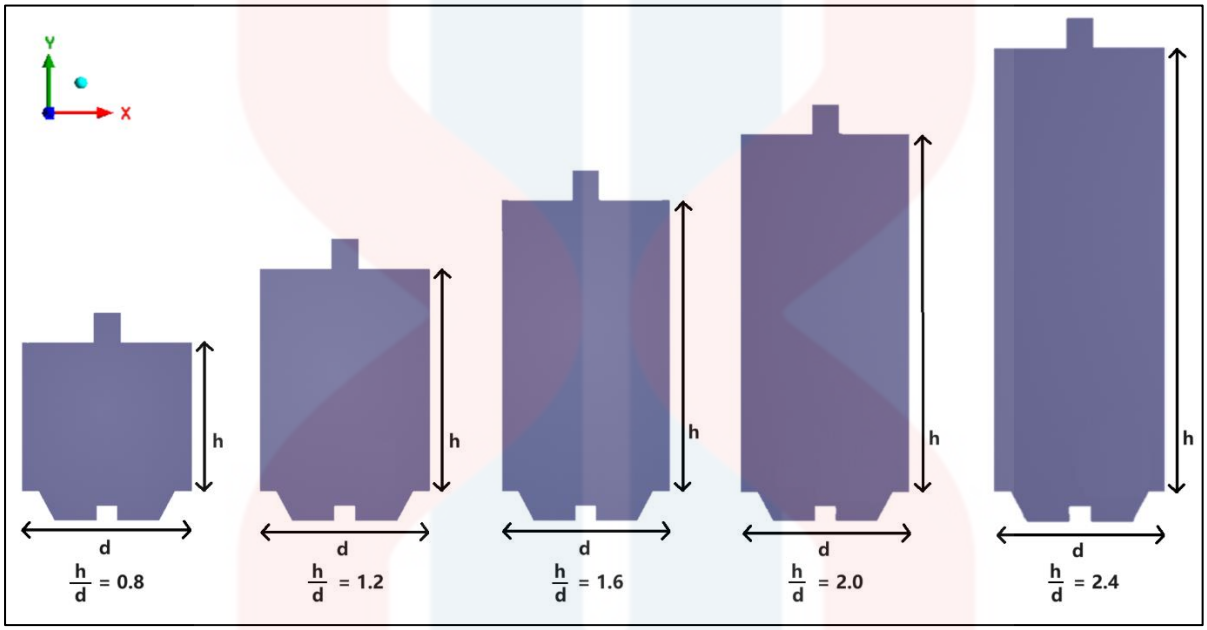

Figure 3.6: Dispenser height geometries

Figure 3.6 depicts the ANSYS Discovery geometry height variants of 4.0 mm, 6.0 mm, 8.0mm, 10.0 mm, and 12.0mm respectively. The dimensionless values (h/d) of the geometries are 0.8, 1.2, 1.6, 2.0, and 2.4 respectively. These geometries will undergo the meshing process in ANSYS Workbench before they are used simulate the LED encapsulation at respective dispenser parameters using ANSYS Fluent where the results are obtained to be studied.

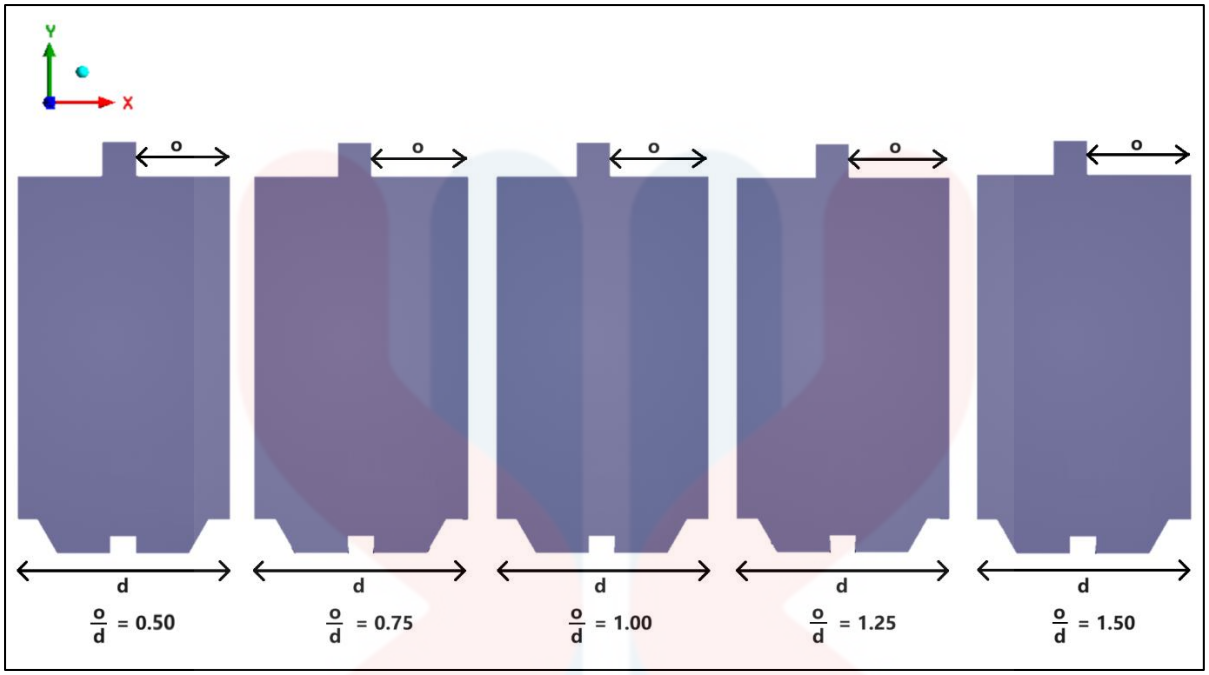

Figure 3.7: Dispenser offset geometries

Figure 3.7 depicts the ANSYS Discovery geometry offset variants of 0.1 mm, 0.15 mm, 0.20 mm, 0.25 mm, and 0.30 mm respectively. The dimensionless values of the geometries are 0.5, 0.75, 1.00, 1.25, and 1.50 respectively. These geometries will undergo the meshing process in ANSYS Workbench before they are used simulate the LED encapsulation at respective dispenser parameters using ANSYS Fluent where the results are obtained to be studied.

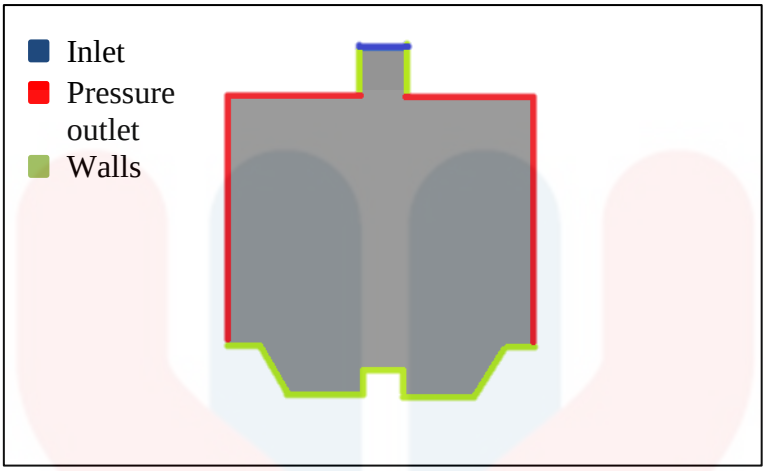

Figure 3.8: Mesh named selections

The various geometries made using ANSYS Discovery were imported into ANSYS Workbench to start the meshing process. Before the meshing process, named selections were made to label the various parts of the 2D geometry. Figures 3.8 depict the named selections of inlet, pressure outlet, and wall respectively. First, the inlet is where parameters such as velocity (m/s) and pressure (Pa) are set to dispense the epoxy resin into the 2D simulation space. Next, pressure outlets are where air pressure is released. In this simulation they are used to simulated open air. Finally, walls are solid objects which epoxy resin can adhere to and interact with in the simulation. The needle's inner walls and LED chip surfaces are labelled as walls appropriately.

Table 3.1: Mesh size, nodes, and elements

Mesh size (mm)	Nodes	Elements
0.10	2496	2388
0.08	3830	3698
0.06	6788	6612
0.04	**15166**	**14852**
0.02	58767	59244

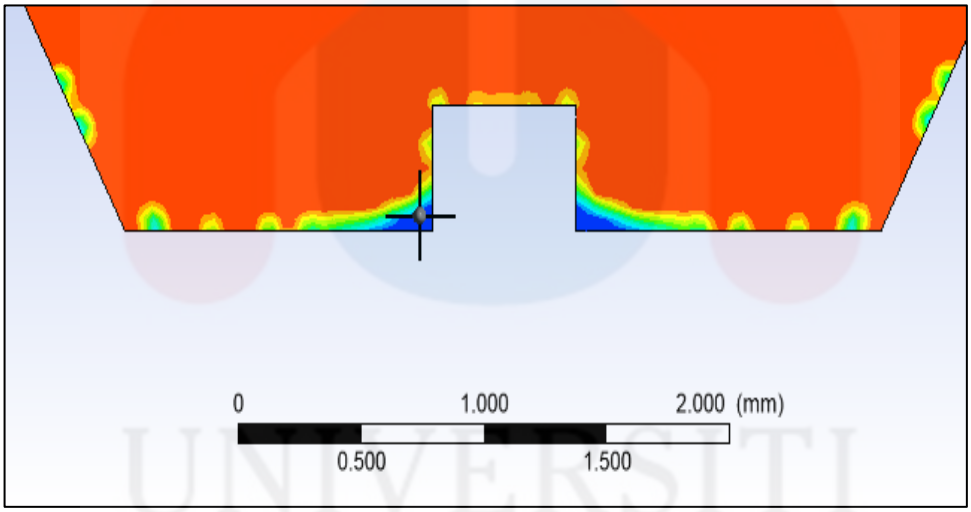

Figure 3.9: Pressure point value

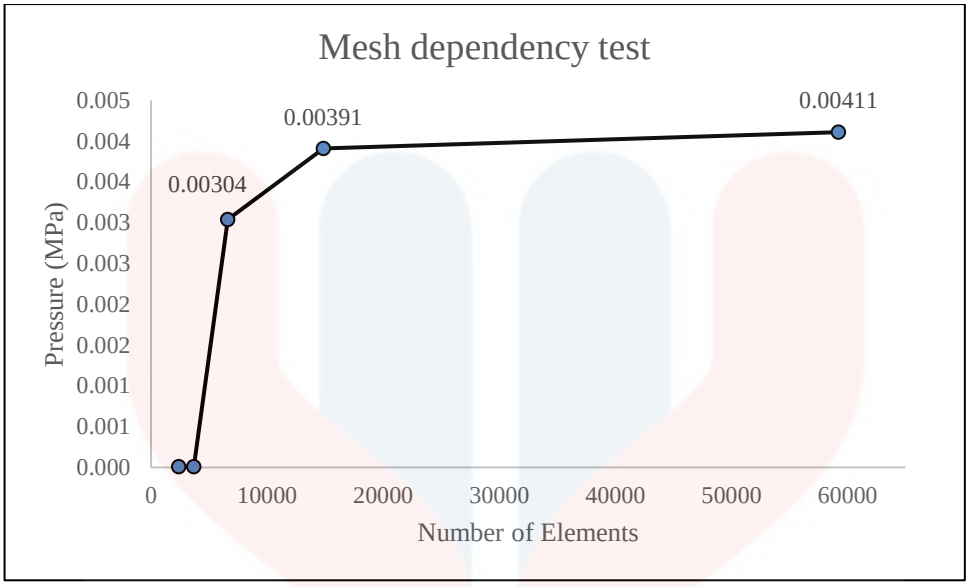

Figure 3.10: Pressure against number of elements

After making the named selections, the geometries were meshed using the face sizing method in ANSYS Workbench to generate a mesh for the simulation process. To determine a suitable mesh size for the geometries, a mesh dependency test was conducted. A mesh dependency test is a crucial step in numerical simulations, especially in computational fluid dynamics (CFD). The purpose of a mesh dependency test is to evaluate the sensitivity of the simulation results to the mesh resolution, or in simpler terms, to determine how much the results change as the mesh size is varied. The process of a mesh dependency test usually involves mesh generation of multiple mesh sizes, simulations, results comparison, and convergence analysis. First, generation of multiple meshes. Several meshes are generated with varying levels of resolution, specifically at 0.10 mm, 0.08 mm, 0.06 mm, 0.04mm, and 0.02mm which covers coarse to fine meshing respectively with the nodes and elements generated tabulated in Table 3.1. Next, simulation runs. The simulations were then run using each determined mesh size with the same boundary conditions, material properties, and other input parameters which were used for each simulation. This is followed by result comparison as the pressure point value results obtained from different meshes are compared. The key output parameter that will be studied for this mesh dependency test is pressure distribution at a point,

as depicted in Figure 3.9. With the pressure point value data obtained from the different meshes, a convergence analysis is done based on the plotted graph using the data as depicted in Figure 3.9. This involves determining if the solution is approaching an asymptotic value as the mesh is refined. Essentially, the convergence analysis is done as an accuracy assessment which helps in evaluating the accuracy of the simulation. If the results change significantly with mesh refinement, it indicates that the solution is not yet converged and may not be reliable. From Figure 3.10, it was determined that there was a significant increase in the pressure point value from element number of 6612 to 14852 which was calculated to be a 28.6% increase. This percentage still increased by 5.12% from element number of 14852 to 59244. With that said, the geometry selection scoping method was used to select the face of the geometry and the mesh size set for the mesh was 0.04mm. This mesh size was used for all the geometry variants to maintain meshing consistency throughout the simulation.

3.2.5 Simulation Procedures

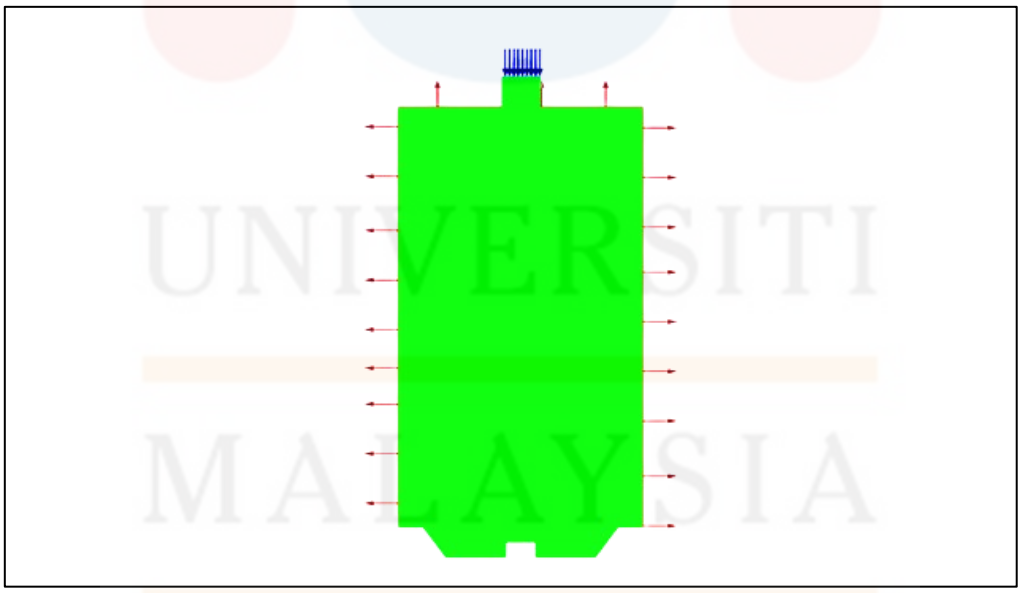

Figure 3.11: Mesh display in ANSYS Fluent

Figure 3.11 depicts the completed ANSYS Workbench geometry mesh display which was imported into ANSYS Fluent. Additionally, the mesh display also depicts the inlet, pressure outlet, and walls of the mesh.

Table 3.2: Fluid material properties

Fluids	Density (kg/m^3)	Viscosity [kg/(m^{-1}s^{-1})]	Phases
Air	1.225	1.7894e-05	Primary
Epoxy resin	1800	0.448	Secondary

Table 3.2 depicts the boundary conditions for fluid material properties which are present in the simulation. The primary phase of the simulation is air, which is set to have a density of 1.225 kg/m^3, and a viscosity of 1.7894e-05 kg/m^{-1}s^{-1}. The secondary phase of the simulation is epoxy resin, which is set to have a density of 1800 kg/m^3, and a viscosity of 0.448 kg/m^{-1}s^{-1}. These fluid material properties are the boundary conditions that will determine the behaviour of these fluids during the ANSYS Fluent simulation. First, density. The density of a fluid is a measure of its mass per unit volume. In this simulation, the density values for air and epoxy resin provide information about how much mass is present in each volume of these fluids. Density affects the buoyancy and the distribution of forces within the fluid domain, influencing the flow patterns and the interaction between the two phases which is crucial for our study into micro void formation. Next, viscosity. Viscosity is a measure of a fluid's resistance to deformation or flow. The viscosity values provided for air and epoxy resin indicate how easily these fluids will deform or flow under the influence of applied forces. In this simulation, viscosity is a key factor in determining the frictional forces within the fluid and influences the overall flow behaviour, including the formation of boundary layers and the dissipation of kinetic energy which are also important towards our study into micro void formations.

Furthermore, the boundary conditions of the ANSYS simulation includes the multiphase model configurations, and viscous model configurations respectively. First, the volume of fluid multiphase model will be used to simulate the primary and secondary phases

which are air and epoxy. The VOF multiphase model is employed to simulate the behaviour of the primary (air) and secondary (epoxy) phases within the computational domain which enables the tracking of phase interfaces and the interaction between distinct fluid phases. The phase interaction between air and epoxy is specified at a constant value of 0.005 N/m which determines the surface tension between the two phases. This parameter influences phenomena such as droplet formation, coalescence, and the overall behaviour of the multiphase system. More importantly, surface tension affects the micro void formation as well.

Besides that, the viscous model utilized in the simulation is k-epsilon with scalable wall functions. This viscous model is employed to characterize the viscous behaviour and turbulence within the fluid domain. The k-epsilon model is widely used for simulating turbulent flows and provides insights into turbulence kinetic energy and its dissipation rate. More crucially, Scalable wall functions are utilized to model the near-wall flow behaviour, allowing for efficient and accurate simulations of boundary layer phenomena and wall-bounded flows. Near-wall flow behaviour in this context also relates to the micro void formations in the LED encapsulation process where the epoxy interacts with the LED chip housing.

To emphasise, these boundary conditions are maintained constant throughout the simulations of all dispenser parameter variants (height, velocity, offset). This consistency is crucial for ensuring reproducibility and comparability of simulation results across different scenarios and conditions. By keeping the boundary conditions constant, the simulations maintain a standardized set of inputs, enabling a systematic exploration of the effects of varying dispenser parameters on the fluid behaviour, micro void formation and system performance.

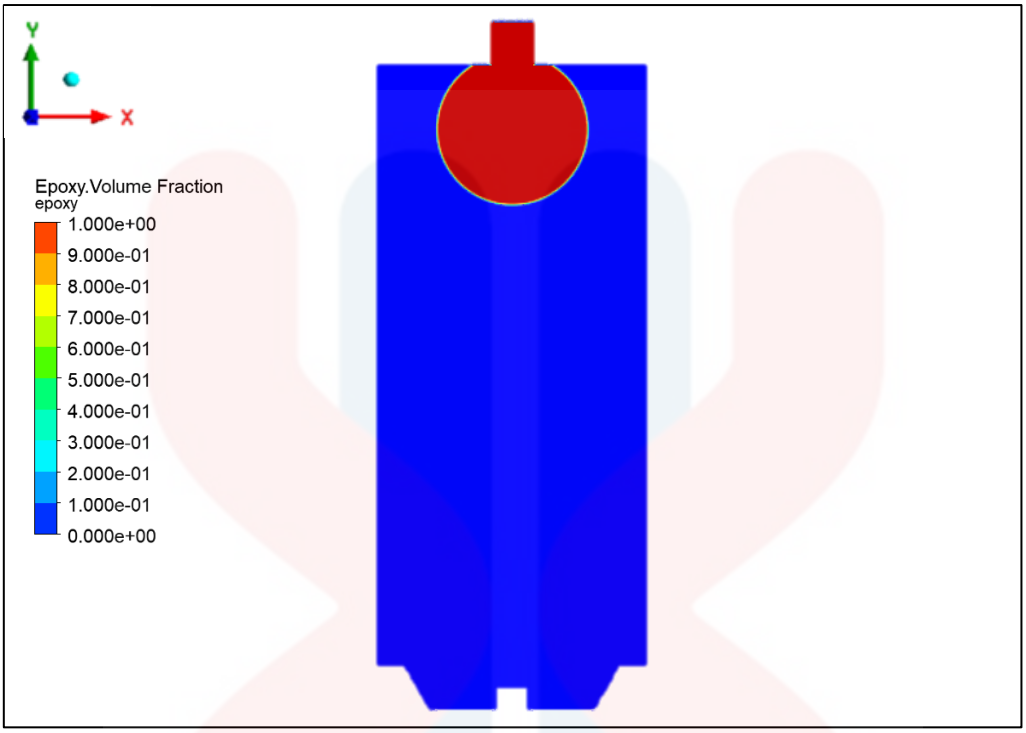

Figure 3.12: Contour of VOF

Figures 3.12 depicts the VOF contour display. First, the region register is utilised to determine a region of cells within the mesh which will be patched with epoxy resin after initialization. Next, solution initialization is done accordingly, and the epoxy droplet region register is patched. Moving forward, the contour configuration was set to display the contour of phases. More specifically, the contour of epoxy VOF was displayed in Figure 3.12. Lastly, calculation was conducted, and the simulation is run until the desired results of micro void formation are acquired. To emphasise, an animation of the epoxy VOF contour and a graph of scaled residuals will be produced and studied. It is important to note that both region register coordinates and number of time steps for calculation are adjusted according to the dispenser parameters of the mesh.

CHAPTER 4

RESULTS AND DISCUSSION

4.1 Validation of Experiment and Simulation

The experiment results obtained from the LED encapsulation dispensing process had given valuable insight into the behaviour of epoxy resin during LED encapsulation which were discussed. Furthermore, the information gathered during the experiment also contributed towards the design of the LED encapsulation simulation in the ANSYS software.

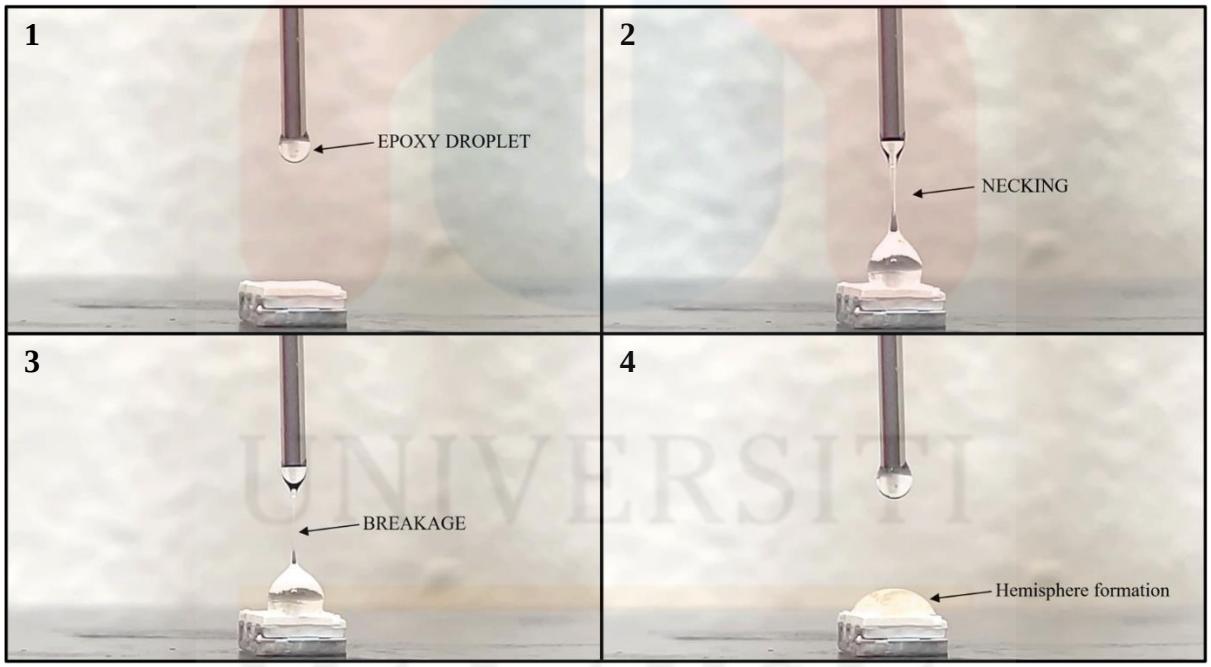

Figure 4.1: Experiment results

Figures 4.1 depicts the results of the LED encapsulation experiment that was conducted in the laboratory. First, application of pressure. The experiment began with the application of pressure to the syringe using the diaphragm pump, leading to the formation of an epoxy droplet, which is the initial stage of encapsulating the LED chip. Next, epoxy droplet growth. The epoxy droplet steadily grew until it reached a point where it started to fall. This growth phase is crucial for ensuring that the LED chip will be adequately encapsulated. Furthermore, necking and elongation. As the droplet fell, necking began to occur between the epoxy residue at the dispensing needle tip and the droplet itself. This necking became thinner as it elongates while the droplet fell. Eventually, breakage. The necking process causes the droplet to become so thin that it breaks at the thinnest point and detaches from the dispenser. Lastly, formation of hemisphere shape. After breakage occurs and the droplet reaches the LED chip, the epoxy droplet settles into a hemisphere shape as it encapsulates the LED chip. This final shape indicates that the LED chip has been successfully encapsulated. These key steps in the LED encapsulation process are observed to validate the simulation results that are obtained later.

Essentially, the deformation and breakage of droplets in airflows is key in various applications of spray and atomization processes (Xu, Wang, & Che, 2020). With that said, the necking and breakage present in the LED encapsulation process is a key factor to be studied as it may also has effects on encapsulant micro void formation. Furthermore, there is also a significant change to the epoxy resin opacity as it turns opaquer with the passing of time referring to Figures 4.1. Comparing the new droplet formation at the dispensing needle tip and the hemisphere formation, From Figure 4.1 it is evident that the epoxy has started to harden quickly throughout the encapsulation process. Simply put, this change in material property needs to be considered when the dispenser parameter is varied as it will affect the encapsulation and micro void formation process significantly due to the longer time taken distance travelled by the epoxy droplet as it hardens.

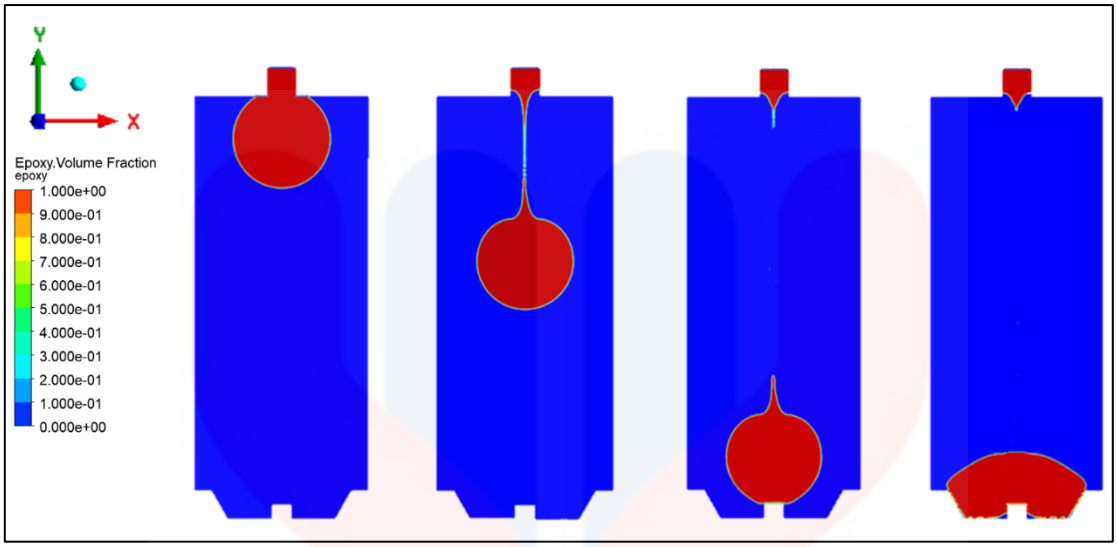

Figure 4.2: Simulation of LED encapsulation

Figure 4.2 depicts the results of LED encapsulation simulation using ANSYS Fluent. First, epoxy droplet patching. The epoxy droplet was patched into the simulation mesh to match the epoxy droplet formed in the experiment with an assumption that the droplet is spherical in shape. This droplet size is crucial for ensuring that the LED chip will be adequately encapsulated during the simulation process. Next, necking and elongation. As the simulation progressed, the droplet fell, and necking began to occur between the epoxy residue at the dispensing needle tip and the droplet itself. This necking became thinner as it elongates while the droplet fell. Eventually, breakage. The necking process causes the droplet to become so thin that it breaks at the thinnest point and detaches from the dispenser. Lastly, formation of hemisphere shape. After breakage occurs and the droplet reaches the LED chip, the epoxy droplet settles into a hemisphere shape as it encapsulates the LED chip. This final shape indicates that the LED chip has been successfully encapsulated. These key steps in the LED encapsulation process were also observed during the experiment process which validates the simulation results.

4.2 Simulation Results

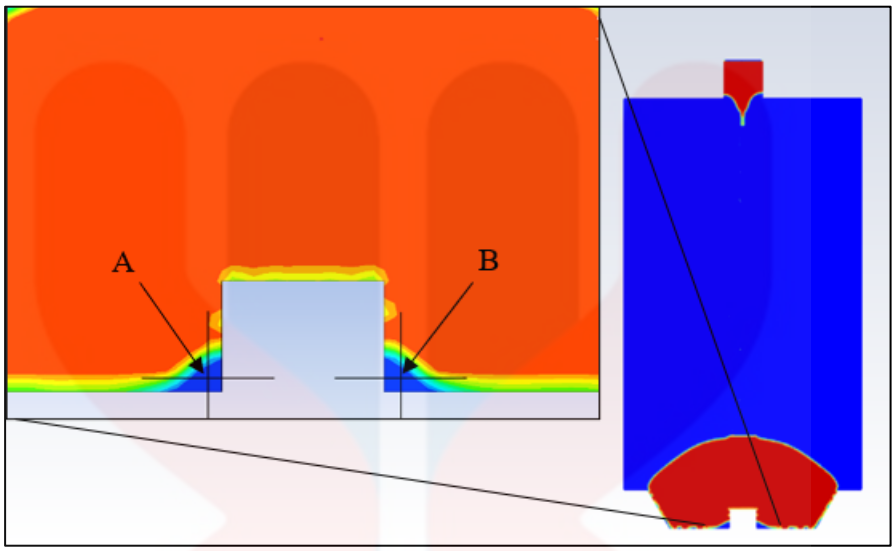

Figure 4.3: VOF point A and B of micro void formation

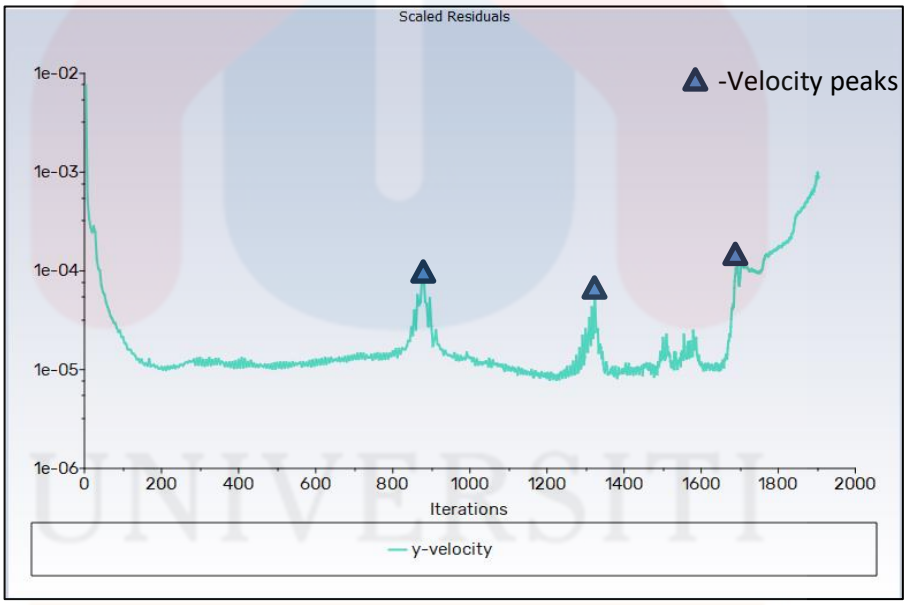

Figure 4.4: Y-velocity scaled residuals graph

The simulation results obtained from the ANSYS Fluent software had given valuable input into the behaviour of epoxy resin during LED encapsulation and micro void formation which were discussed. Furthermore, the flow visualisation of epoxy droplets was also noted through the ANSYS Fluent simulations of various LED encapsulant dispenser parameters such as height, velocity, and offset. This flow visualisation includes the understanding of how the epoxy resin flows, spreads, and interacts with various components within the encapsulation

setup, such as the LED chip, substrate, and surrounding walls. By analysing the flow patterns and dynamics, the simulations can offer critical information about the behaviour of the epoxy resin and micro void formation during the encapsulation process. Figure 4.3 depicts the simulation VOF point values A and B which were tabulated and analysed to study the formation of micro voids during the simulated LED encapsulation process. By analysing the VOF (Volume of Fluid) point values A and B, the occurrence and behaviour of micro voids within the resin can be studied and quantified. Understanding the formation of micro voids is essential for assessing the quality and integrity of the encapsulation, as well as identifying potential areas for improvement in the manufacturing process. Additionally, the simulations allow for the visualization of epoxy droplets and micro void within the LED encapsulation setup. By varying parameters such as dispenser height, velocity, and offset, the behaviour of the epoxy droplets and micro void formation could be observed and analysed. This provides valuable insights into how different dispenser parameters impact the distribution, deposition, and micro void formation of epoxy resin, aiding in observation and study of the encapsulation process for consistent and uniform results. Figure 4.4 depicts the y-velocity scaled residuals graph of the simulations which demonstrates the changes in velocity that occurred in the simulation. The 3 distinct peaks marked on the graph are the epoxy velocity changes when it is met with a wall. More specifically, the epoxy resin experienced a change in velocity when it hit the LED chip, substrate, and side walls respectively. This analysis is crucial for understanding how the epoxy resin interacts with the components, experiences velocity variations, and how these factors impact the micro void formation in the encapsulation process.

4.2.1 Dispenser Height

First, the dispenser height and point values of the simulations run with the parameter of varying dispenser heights were recorded. The dispenser height variations chosen for this parameter were 4.0 mm, 6.0 mm, 8.0 mm, 10.0 mm, 12.0 mm. This means that the distance between the LED and the dispenser needle are varied for this parameter. The point values of A and B were taken from the simulation results of varying dispenser heights using the probe function with the coordinates of x: -0.32 and y: -0.78 in ANSYS post-processing. The point values were tabulated, and a graph is generated as follows to depict change in micro void size.

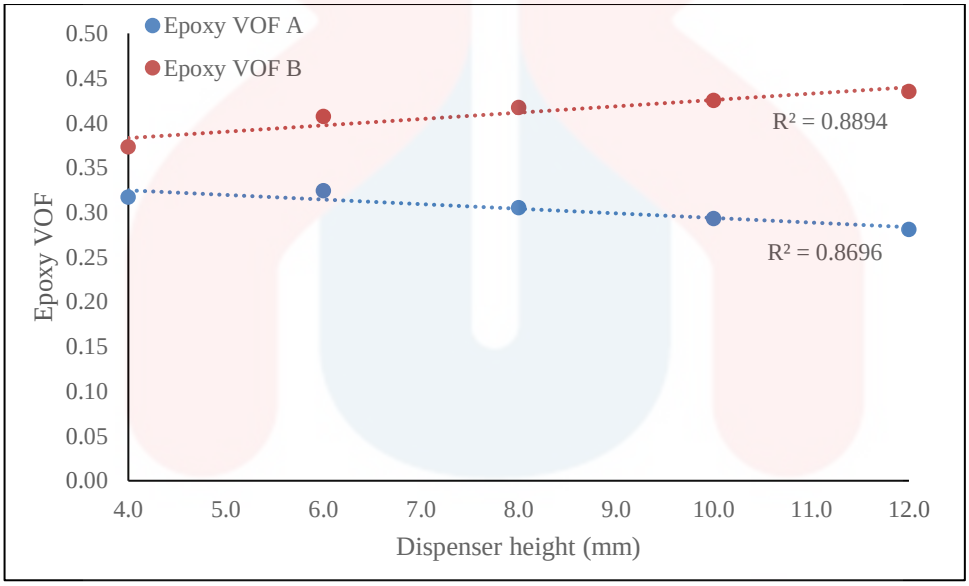

Figure 4.5: Graph of epoxy VOF values against dispenser height

Figure 4.5 depicts the graph generated for the VOF (epoxy) values of dispenser against varying heights. From the graph, an increase in the epoxy VOF values is recorded in point B as the dispenser height is increased. More specifically, the increase in epoxy VOF values in percentages are 9.1%, 2.46%, 1.92%, 2.35%. The R^2 values of Epoxy VOF A and B are 0.8894 and 0.8696 respectively. Essentially, this means that there is a decrease in micro void size with the increase in dispenser height at point B. This implies that as the dispenser height increases, the epoxy fills the voids more completely, resulting in a reduction in micro void size in point B. This relationship suggests that the dispenser height has an impact on the quality and

completeness of the epoxy filling, with higher dispenser heights leading to a more thorough filling and, consequently, smaller micro voids. In practical terms, this information could be important for optimizing the process of epoxy filling, as it indicates that adjusting the dispenser height can influence the quality of the filling and the size of micro voids within the encapsulation material.

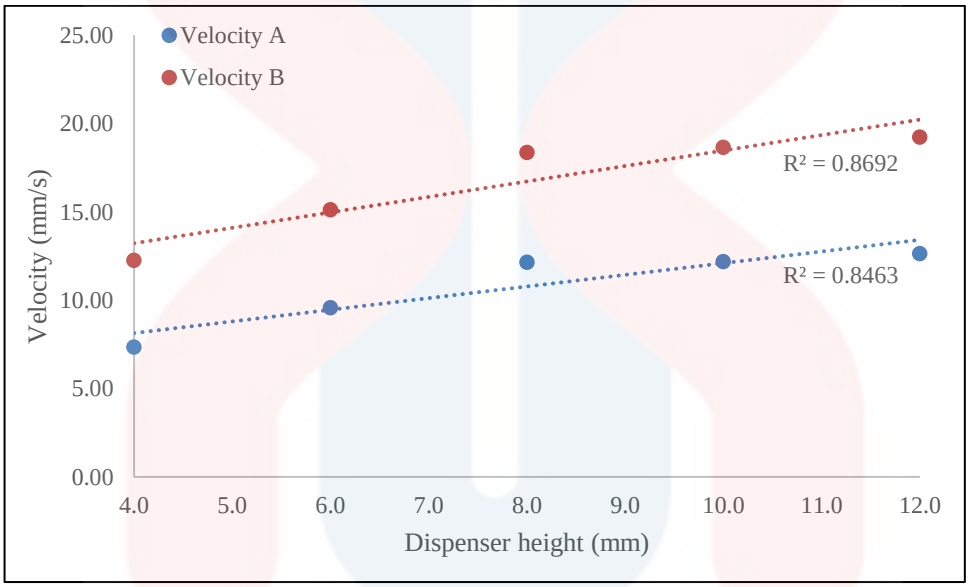

Figure 4.6: Graph of velocity against dispenser height

Figure 4.6 depicts the graph of velocity against dispenser height which was generated from the velocity point values of the ANSYS simulation run with the varying height parameters. From the graph, an increase in velocity is recorded in both points A and B as the dispenser height is increased. More specifically, the increase in point A's velocity values in percentages are 30.21%, 27.03%, 0.25%, and 3.67% respectively. For point B, the increase in velocity values in percentages are 23.31%, 21.45%, 1.59%, and 3.18% respectively. The R^2 of velocity A and B are 0.8463 and 0.8692 respectively. Essentially, this means that there is an increase in epoxy velocity with the increase in dispenser height at point A and B. From this result, it is implied that an increase in dispenser height increases the velocity of epoxy resin which in turn decreases the size of micro void during the LED encapsulation process.

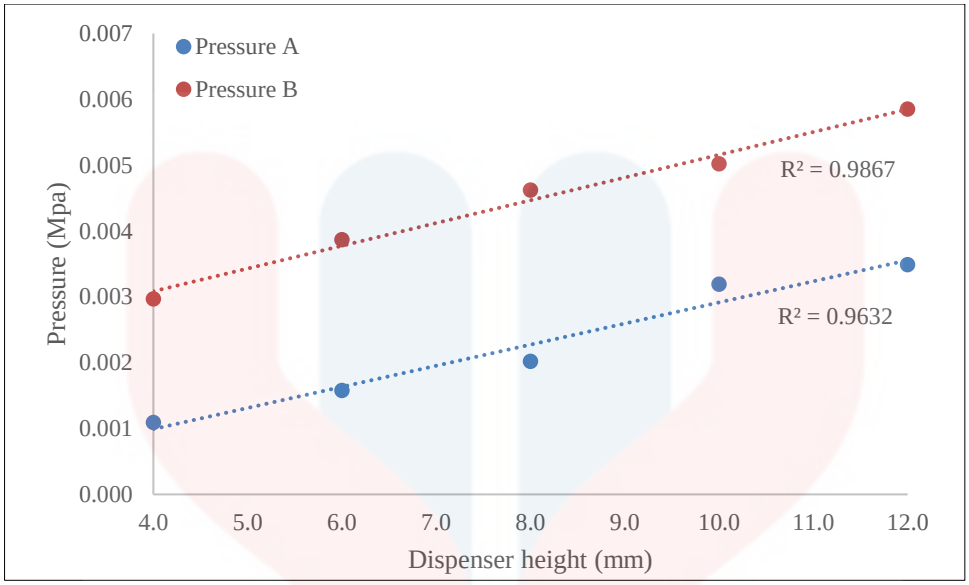

Figure 4.7: Graph of pressure against dispenser height

Figure 4.7 depicts the graph of pressure against dispenser height which was generated from the pressure point values of the ANSYS simulation run with the varying height parameters. From the graph, an increase in pressure is recorded in both points A and B as the dispenser height is increased. More specifically, the increase in point A's pressure values in percentages are 45.0%, 27.8%, 58.4%, and 9.4% respectively. For point B, the increase in pressure values in percentages are 30.3%, 19.4%, 8.66%, and 16.5% respectively. The R^2 values of pressure A and B are 0.9632 and 0.9867 respectively. Essentially, this means that there is an increase in epoxy pressure with the increase in dispenser height at point A and B. From this result, it is implied that an increase in dispenser height increases the pressure of epoxy resin which in turn decreases the size of micro void during the LED encapsulation process.

Next, the time steps and time taken with dispenser height were studied to determine the relationship between dispenser height and time taken to complete encapsulation. The time steps refer to the number of time steps taken for the simulation to complete the LED encapsulation process for each dispenser height. These time steps can be multiplied by the time step size (1e-05) to get the time taken(s) to complete the LED encapsulation process. The graph of time taken, and dispenser height is as follows.

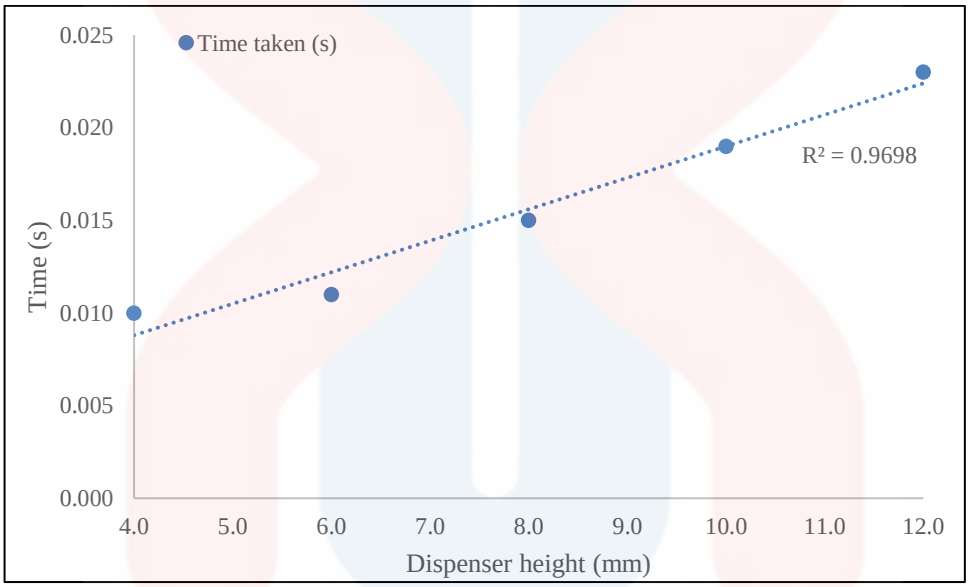

Figure 4.8: Graph of time taken against dispenser height

Figure 4.8 depicts the graph of dispenser height and time taken(s) to complete the LED encapsulation process in the simulation. From the graph, it is evident that as the dispenser height increase, the time taken for the LED encapsulation to complete in simulation is increased. From the obtained data, it is determined that a dispenser height of 8.0 mm is the preferred dispenser height for the ANSYS simulation of LED encapsulation. This is justified because the increase in dispenser height from 8.0mm to 10.0mm only increased the epoxy VOF value by 1.92% but increases the time taken of LED encapsulation by 0.004s. The R^2 value time taken is 0.9698. With that said, the dispenser height for the following parameters of velocity and offset will be set at 8.0mm.

4.2.2 Dispenser Velocity

Another parameter that was studied was dispenser velocity. The dispenser velocity and point values of the simulations run with the parameter of varying dispenser velocity were recorded. The dispenser velocity variations chosen for this parameter were 0.3 m/s, 0.4 m/s, 0.5 m/s, 0.6 m/s, 0.7 m/s. This means that the initial velocity of the epoxy dispenser is varied for the study of this parameter. The point values of A and B are taken from the simulation results of varying dispenser velocity using the probe function with the coordinates of x: -0.32 and y: -0.78 in ANSYS post-processing. The point values were tabulated, and a graph is generated as follows to depict the change in micro void size.

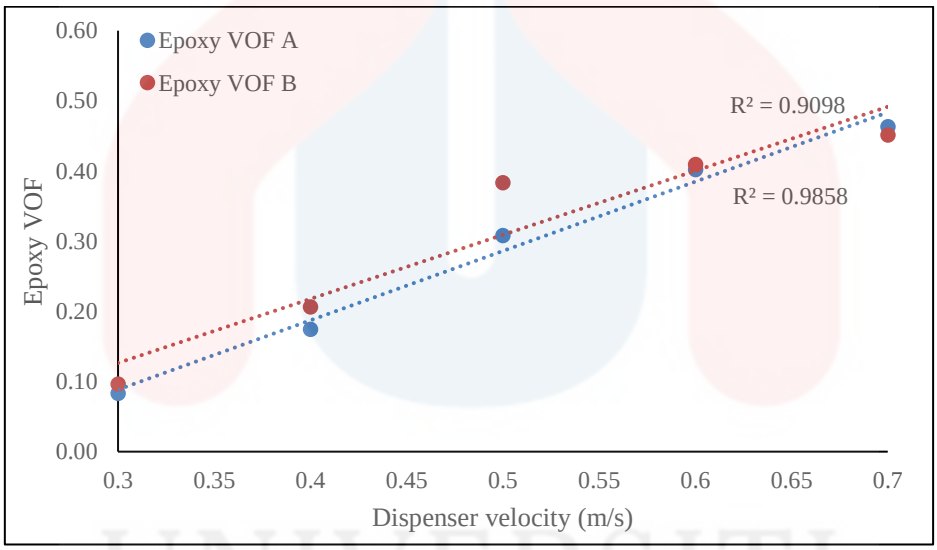

Figure 4.9: Graph of epoxy VOF values against dispenser velocity

Figure 4.9 depicts the graph generated for the VOF (epoxy) values of dispenser against varying velocities. From the graph, an increase in the epoxy VOF values is recorded in both point A and B as the dispenser velocity is increased. More specifically, the increase in epoxy VOF values in percentages are 109.64%, 76.72%, 30.52%, and 15.17% for point A. For point B, the increase of epoxy VOF values in percentages are 114.58%, 85.92%, 6.80%, and 10.26%. The R^2 values of Epoxy VOF A and B are 0.9858 and 0.9098 respectively. Essentially, this means that there is a decrease in micro void size with the increase in dispenser velocity. This implies that as the dispenser velocity increases, the epoxy fills the voids more completely,

resulting in a reduction in micro void size. This relationship suggests that the dispenser velocity has an impact on the quality and completeness of the epoxy filling, with higher dispenser velocities leading to a more thorough filling and, consequently, smaller micro voids. In practical terms, this information could be important for optimizing the process of epoxy filling, as it indicates that adjusting the dispenser velocity can influence the quality of the filling and the size of micro voids within the encapsulation material.

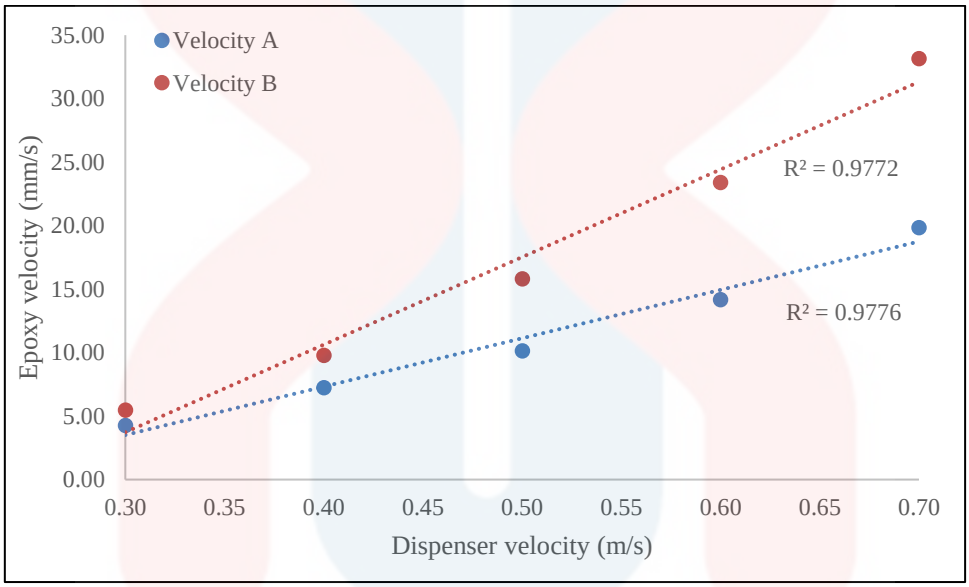

Figure 4.10: Graph of epoxy velocity against dispenser velocity

Figure 4.10 depicts the graph of epoxy velocity against dispenser velocity which was generated from the velocity point values of the ANSYS simulation run with the varying dispenser velocity parameters. From the graph, an increase in velocity is recorded in both points A and B as the dispenser velocity is increased. More specifically, the increase in point A's velocity values in percentages are 69.79%, 40.10%, 39.80%, and 39.89% respectively. For point B, the increase in velocity values in percentages are 78.97%, 61.49%, 47.95%, and 41.72% respectively. The R^2 values of velocity A and B are 0.9776 and 0.9772 respectively. Essentially, this means that there is an increase in epoxy velocity with the increase in dispenser velocity at point A and B. From this result, it is implied that an increase in dispenser velocity

increases the velocity of epoxy resin which in turn decreases the size of micro void during the LED encapsulation process.

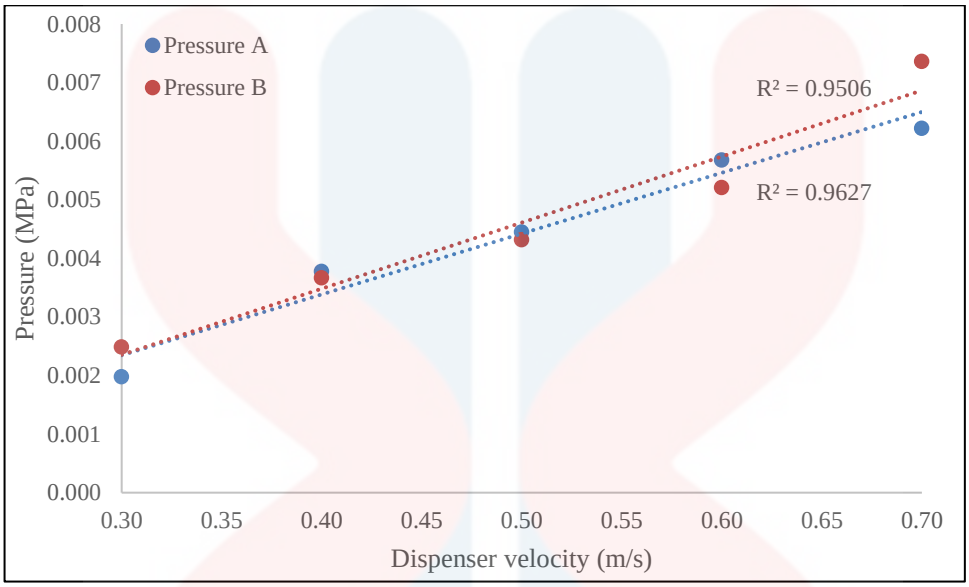

Figure 4.11: Graph of pressure against dispenser velocity

Figure 4.11 depicts the graph of pressure against dispenser velocity which was generated from the pressure point values of the ANSYS simulation run with the varying dispenser velocity parameters. From the graph, an increase in pressure is recorded in both points A and B as the dispenser velocity is increased. More specifically, the increase in point A's pressure values in percentages are 91.01%, 16.67%, 27.73%, and 9.51% respectively. For point B, the increase in pressure values in percentages are 47.19%, 17.75%, 20.95%, and 41.28% respectively. The R^2 values of pressure A and B are 0.9627 and 0.9506 respectively. Essentially, this means that there is an increase in epoxy pressure with the increase in dispenser velocity at point A and B. From this result, it is implied that an increase in dispenser velocity increases the pressure of epoxy resin which in turn decreases the size of micro void during the LED encapsulation process.

Next, the time steps and time taken with dispenser velocity were studied to determine the relationship between dispenser velocity and time taken to complete encapsulation. The time

steps tabulated refer to the number of time steps taken for the simulation to complete the LED encapsulation process for each dispenser velocity. These time steps can be multiplied by the time step size (1e-05) to get the time taken(s) to complete the LED encapsulation process. The graph of time taken, and dispenser velocity is as follows.

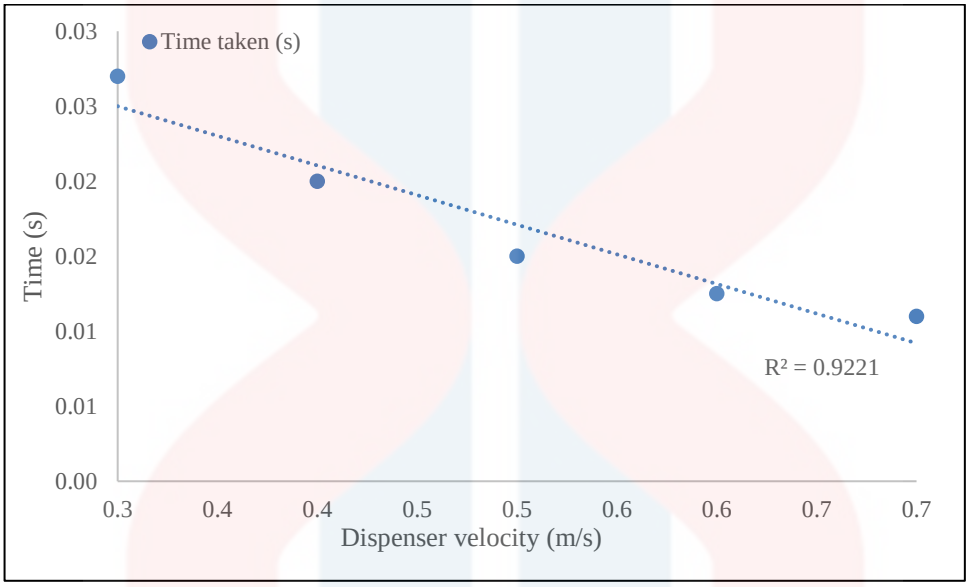

Figure 4.12: Graph of time taken against dispenser velocity

Figure 4.12 depicts the graph of dispenser velocity and time taken(s) to complete the LED encapsulation process in the simulation. From the graph, it is evident that as the dispenser velocity increases, the time taken for the LED encapsulation to complete in simulation is decreased. From the obtained data, it is determined that a dispenser velocity of 0.6 m/s is the preferred dispenser velocity for the ANSYS simulation of LED encapsulation. This is justified because the increase in dispenser height from 0.6 m/s to 0.7 m/s only increased the epoxy VOF value by 15.17% at point A and 10.26% at point B while only decreasing the time taken of LED encapsulation by 0.002s. The R^2 value of time taken is 0.9221. With that said, the dispenser velocity for the following parameter of offset will be set at 0.6 m/s.

4.2.3 Dispenser Offset

Furthermore, the dispenser offset parameter was also simulated and studied. The dispenser offset and point values of the simulations run with the parameter of varying dispenser offset were recorded. The dispenser offset variations chosen for this parameter were 0.10 mm, 0.15 mm, 0.20 mm, 0.25 mm, 0.30 mm. This means that the offset of the epoxy dispenser from point B is varied for the study of this parameter. The point values of A and B are taken from the simulation results of varying dispenser offset using the probe function with the coordinates of x: -0.32 and y: -0.78 in ANSYS post-processing. The point values were tabulated as demonstrated, and a graph is generated as follows to depict the change in micro void size.

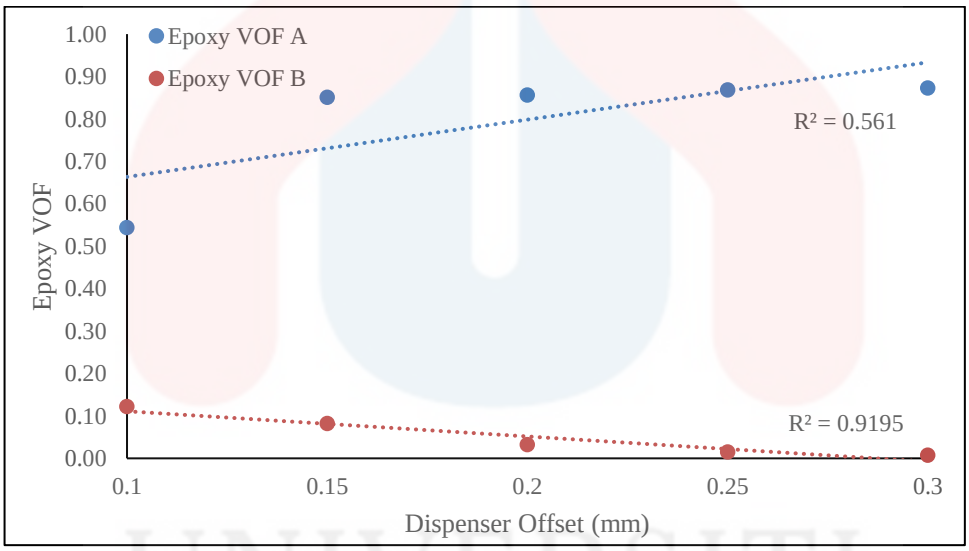

Figure 4.13: Graph of epoxy VOF values and dispenser offset

Figure 4.13 depicts the graph generated for the VOF (epoxy) values of dispenser against varying offset. From the graph, an increase in the epoxy VOF values is recorded in point A while a decrease in VOF is recorded in point B as the dispenser offset is increased. More specifically, the increase in epoxy VOF values in percentages are 56.43%, 0.59%, 1.40%, and 0.58% for point A. For point B, the decrease of epoxy VOF values in percentages are 32.79%, 60.98%, 53.13%, and 53.33%. The R^2 values of epoxy VOF A and B are 0.561 and 0.9195 respectively. Essentially, this means that there is a decrease in micro void size at point A with the increase in dispenser offset from point B. This implies that as the dispenser offset

increases from point B, the epoxy fills the voids more completely in point A, resulting in a reduction in micro void size in point A. This relationship suggests that the dispenser offset has an impact on the quality and completeness of the epoxy filling at a point, with higher dispenser offset leading to a more thorough filling and, consequently, smaller micro voids at a point. In practical terms, this information could be important for optimizing the process of epoxy filling, as it indicates that adjusting the dispenser velocity can influence the quality of the filling and the size of micro voids within the encapsulation material.

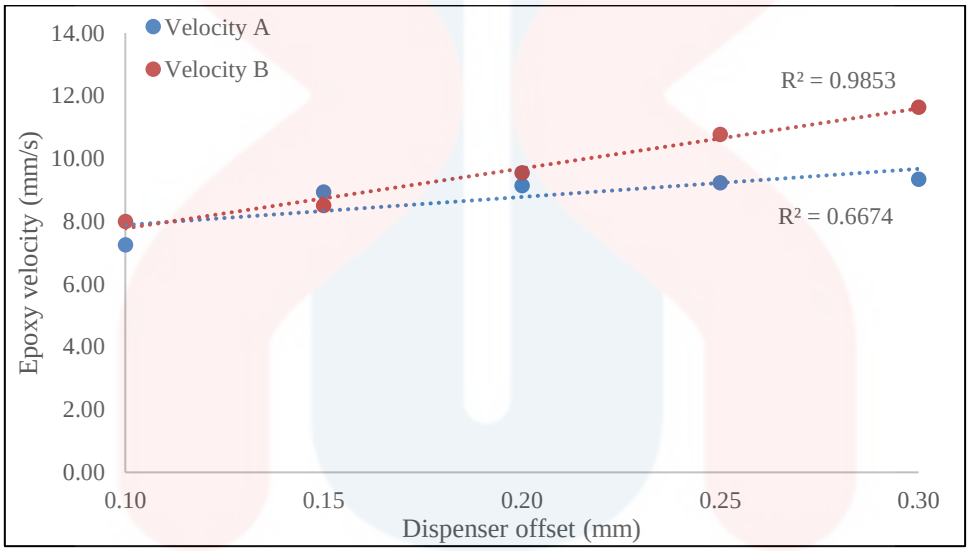

Figure 4.14: Graph of epoxy velocity against dispenser offset

Figure 4.14 depicts the graph of velocity against dispenser offset which was generated from the velocity point values of the ANSYS simulation run with the varying dispenser offset parameters. From the graph, point A's velocity remained stable while an increase in velocity is recorded in point B was as the dispenser offset is increased. More specifically, the increase in point A's velocity values in percentages are 23.03%, 2.36%, 1.00%, and 1.17% respectively. For point B, the increase in velocity values in percentages are 6.43%, 12.21%, 12.88%, and 8.04% respectively. The R^2 values of velocity A and B are 0.6674 and 0.9853 respectively. Essentially, this means that there is an increase in epoxy velocity at point B with the increase in dispenser offset from point B. From this result, it is implied that an increase in dispenser

offset stabilises the velocity of epoxy resin which in turn decreases the size of micro void at point A during the LED encapsulation process.

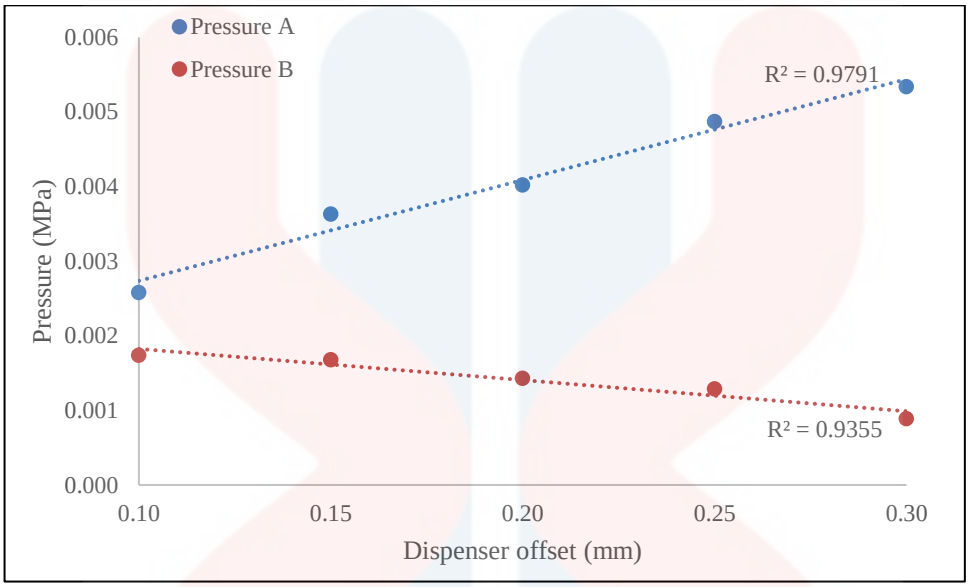

Figure 4.15: Graph of pressure against dispenser offset

Figure 4.15 depicts the graph of pressure against dispenser offset which was generated from the pressure point values of the ANSYS simulation run with the varying dispenser offset parameters. From the graph, an increase in pressure is recorded in point A while a pressure drop was recorded in point B as the dispenser offset is increased. More specifically, the increase in point A's pressure values in percentages are 40.70%, 10.73%, 21.14%, and 9.65% respectively. For point B, the drop in pressure values in percentages are 3.45%, 14.88%, 9.79%, and 31.01% respectively. The R^2 values of pressure A and B are 0.9791 and 0.9355 respectively. Essentially, this means that there is an increase in epoxy pressure with the increase in dispenser offset at point A while there was a decrease in epoxy pressure at point B. From this result, it is implied that an increase in dispenser offset increases the pressure of epoxy resin which in turn decreases the size of micro void at point A during the LED encapsulation process.

Next, the time steps and time taken with dispenser offset were studied to determine the relationship between dispenser height and time taken to complete encapsulation. The time steps tabulated refers to the number of time steps taken for the simulation to complete the LED encapsulation process for each dispenser offset. These time steps can be multiplied by the time step size (1e-05) to get the time taken(s) to complete the LED encapsulation process. The graph of time taken, and dispenser offset is as follows.

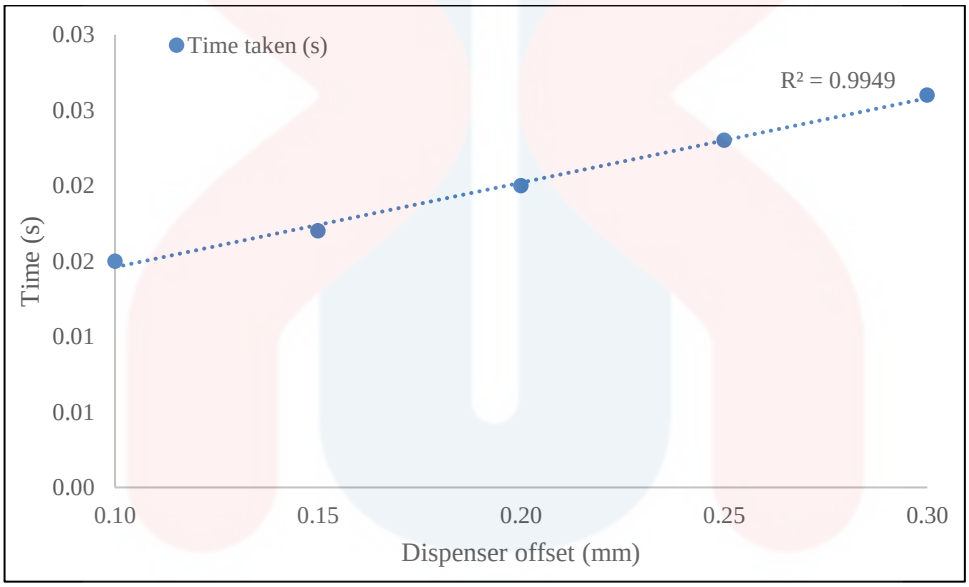

Figure 4.16: Graph of time taken against dispenser offset

Figure 4.16 depicts the graph of dispenser offset and time taken(s) to complete the LED encapsulation process in the simulation. From the graph, it is evident that as the dispenser offset increases, the time taken for the LED encapsulation to complete in simulation is increased. From the obtained data, it is determined that a dispenser offset of 0.2 mm is the preferred dispenser offset for the ANSYS simulation of LED encapsulation. This is justified because the increase in dispenser height from 0.20 mm to 0.25 mm only increased the epoxy VOF value by 1.40% at point A and decrease by 53.13% at point B while increasing the time taken of LED encapsulation by 0.003s. The R^2 value of time taken is 0.9949.

4.2.4 Effects of Dispenser Parameters on Micro Void Formation

From the simulation results, it is shown that the effects of dispenser parameters, specifically height, velocity, and offset on the LED encapsulation process can significantly impact the micro void formation and efficiency of the encapsulation process. First, dispenser height. The dispenser height plays a crucial role in determining the consistency of material dispensing onto the LED chip. A shorter needle height, such as 4.0mm, may provide more precise control and finer dispensing, while a taller needle height, such as 12.0mm, may allow for greater material flow but with potentially less precision due to splashing and spray. Understanding the impact of needle height on the consistency of material deposition is essential for achieving uniform encapsulation across LED components. Next, velocity. The dispenser velocity can affect the potential for air entrapment and void formation within the encapsulation material. A higher velocity may reduce the likelihood of air entrapment due to more controlled dispensing, while a low velocity could potentially result in increased air entrapment, especially in viscous encapsulation materials. This air entrapment is the main factor for micro void formations within the encapsulation material. Furthermore, dispenser offset. From the simulation, dispenser offset from point B has caused larger micro void formations which was observed from probing point values from point B with increasing offset distance. Understanding how dispenser parameters such as height, velocity, and offset influences the prevention of air entrapment and void formation which is critical for minimizing defects in the encapsulation process. The selection of dispenser parameters can impact process throughput and cycle time. A shorter needle height may allow for faster material dispensing and higher throughput due to decreased distance between LED housing and dispensing needle.

CHAPTER 5

CONCLUSION AND RECOMMENDATIONS

5.1 Conclusion

Conclusively, micro void formation analysis of LED encapsulation using epoxy resin was conducted using ANSYS Fluent Computational Fluid Dynamics (CFD). The micro void formation analysis enables the identification of different dispensing parameter's effects on the micro void formation in LED encapsulant. The dispenser needle and LED chip were modelled after the components used in the physical experiment.

Essentially, the choice of dispenser needle parameters in the LED encapsulation process has multifaceted effects on material dispensing consistency, encapsulation quality, air entrapment, and process efficiency. Careful consideration of these factors is essential to reduce micro void formation in the LED encapsulation process. Conducting systematic experimentation and process visualisation studies such as the ANSYS Fluent analyses conducted in this project can provide valuable insights into the effects of dispenser parameters on micro void formation during the LED encapsulation process. Specifically, 109.64%, 76.72%, 30.52%, and 15.17% increases in epoxy VOF when velocity was increased, indicating the cruciality of velocity parameter

Therefore, the objectives of validating CFD simulation results via experimental results and investigating the effects of dispenser parameters and formations of micro void in the LED chip encapsulation process using CFD simulation (ANSYS) were met successfully through the conduct of this project.

5.2 Recommendations

Firstly, there are improvements that could be done to improve the physical experimentation for the LED encapsulation. More specifically, the experiment should be done in a vacuum chamber further remove contaminant particles from the encapsulation environment, maintain a constant pressure, and minimise airflow during encapsulation. Additionally, observations of the cured epoxy resin encapsulant could be done using a Scanning Electron Microscope to further study the micro voids formed during the encapsulation process.

Besides that, further analysis can also be done in simulation such as the structural and optical analyses of LED encapsulant affected by micro voids. These are suitable analyses that can be done on LED encapsulants to further study the effects of micro voids on the structural and optical performances of LED encapsulants via Computational Fluid Dynamics (CFD) simulation methods. The simulation should also be done in 3D model but given a more appropriate time allocation and resources for simulation and skills required to do so. A 3D model will provide a more detailed look into the formation of micro voids in the LED encapsulant.

Lastly, a more in-depth subject on the ANSYS software should also be offered by Universiti Malaysia Kelantan to future students undertaking material technology. By offering a subject on the ANSYS software, students can implement and apply knowledge learnt from EFT1252 Computer Application in Design and advance further in their studies into the technology involved in material analyses in our current day. To emphasise, the implementation of an ANSYS subject will allow students to have an in-depth understanding of material properties and behaviour in software simulations.

REFERENCES

Abas, A., Ng, F. C., Gan, Z. L., Ishak, M. H. H., Abdullah, M. Z., & Chong, G. Y. (2018). *Effect of scale size, orientation type and dispensing method on void formation in the CUF encapsulation of BGA*. https://doi.org/10.1007/s12046-018-0849-3

Alim, M. A., Abdullah, M. Z., Aziz, M. S. A., & Kamarudin, R. (2021). Die attachment, wire bonding, and encapsulation process in LED packaging: A review. *Sensors and Actuators, A: Physical*, *329*. https://doi.org/10.1016/j.sna.2021.112817

Alim, Md. A., Abdullah, M. Z., Kamarudin, R., Rusdi, M. S., Ishak, M. I., & Gunnasegaran, P. (2022). *Effect of Needle Size and Needle Height to Substrate in Encapsulation Process of LED Packaging*. 149–156. https://doi.org/10.1007/978-3-030-92964-0_15

Bae, J. Y., Kim, H. Y., Lim, Y. W., Kim, Y. H., & Bae, B. S. (2016). Optically recoverable, deep ultraviolet (UV) stable and transparent sol-gel fluoro siloxane hybrid material for a UV LED encapsulant. *RSC Advances*, *6*(32), 26826–26834. https://doi.org/10.1039/c6ra01346e

Carotti, L., Potente, G., Pennisi, G., Ruiz, K. B., Biondi, S., Crepaldi, A., … Fabiana Antognoni. (2021). Pulsed led light: Exploring the balance between energy use and nutraceutical properties in indoor-grown lettuce. *Agronomy*, *11*(6). https://doi.org/10.3390/agronomy11061106

Chiang, T. H., Lin, Y. C., Chen, Y. F., & Chen, E. Y. (2016). Effect of anhydride curing agents, imidazoles, and silver particle sizes on the electrical resistivity and thermal conductivity in the silver adhesives of LED devices. *Journal of Applied Polymer Science*, *133*(26). https://doi.org/10.1002/app.43587

Gao, N., Liu, W., Yan, Z., & Wang, Z. (2013). Synthesis and properties of transparent cycloaliphatic epoxy-silicone resins for opto-electronic devices packaging. *Optical Materials*, *35*(3), 567–575. https://doi.org/10.1016/j.optmat.2012.10.023

Janai, M., Woon, K. L., & Chan, C. S. (2018). Design of efficient blue phosphorescent bottom emitting light emitting diodes by machine learning approach. *Organic Electronics*, *63*, 257–266. https://doi.org/10.1016/j.orgel.2018.09.029

Kosai, S., Badin, A. B., Qiu, Y., Matsubae, K., Suh, S., & Yamasue, E. (2021). Evaluation of resource use in the household lighting sector in Malaysia considering land disturbances through mining activities. *Resources, Conservation and Recycling*, *166*. https://doi.org/10.1016/j.resconrec.2020.105343

Lin, Z., Mcnamara, A., Liu, Y., Moon, K. sik , & Ping Wong, C. (2014). Exfoliated hexagonal boron nitride-based polymer nanocomposite with enhanced thermal conductivity for electronic encapsulation. *Composites Science and Technology*, *90*, 123–128. https://doi.org/10.1016/j.compscitech.2013.10.018

Lu, Q., Yang, Z., Meng, X., Yue, Y., Ahmad, M. A., Zhang, W., … Chen, W. (2021). A review on encapsulation technology from organic light emitting diodes to organic and perovskite solar cells. *Advanced Functional Materials*, *31*(23). https://doi.org/10.1002/adfm.202100151

Luo, X., Hu, R., Liu, S., & Wang, K. (2016). Heat and fluid flow in high-power LED packaging and applications. *Progress in Energy and Combustion Science*, *56*, 1–32. https://doi.org/10.1016/j.pecs.2016.05.003

Luo, X., & Qiu, C.-W. (2014). *Chip packaging: encapsulation of nitride LEDs*. 441–481. https://doi.org/10.1533/9780857099303.2.441

Nair, G. B., Swart, H. C., & Dhoble, S. J. (2020). A review on the advancements in phosphor-converted light emitting diodes (pc-LEDs): Phosphor synthesis, device fabrication and characterization. *Progress in Materials Science*, *109*. https://doi.org/10.1016/j.pmatsci.2019.100622

Pecht, M., Das, D. B., & Chang, M.-H. (2014). *Introduction to LED Thermal Management and*

Reliability. 3–14. https://doi.org/10.1007/978-1-4614-5091-7_1

Raypah, M. E., Sodipo, B. K., Devarajan, M., & Sulaiman, F. (2016). Estimation of luminous flux and luminous efficacy of low-power SMD LED as a function of injection current and ambient temperature. *IEEE Transactions on Electron Devices*, *63*(7), 2790–2795. https://doi.org/10.1109/TED.2016.2556079

Roslan, H., Aziz, A., Abdullah, M. Z., R. Kamarudin, M. H.H. Ishak, Ismail, F., & Agustinus Purna Irawan. (2020). Analysis of LED wire bonding during encapsulation process. *IOP Conference Series: Materials Science and Engineering*, *1007*(1). IOP Publishing Ltd. https://doi.org/10.1088/1757-899X/1007/1/012173

Ruan, K., Zhong, X., Shi, X., Dang, J., & Gu, J. (2021). Liquid crystal epoxy resins with high intrinsic thermal conductivities and their composites: A mini-review. *Materials Today Physics*, *20*. https://doi.org/10.1016/j.mtphys.2021.100456

Saurabh, G., Animesh, G., Lalit, G., & Khandait, P. D. (2020). Automatic mechanism for LED parameters testing and checking. *IEEE Applied Power Electronics Conference and Exposition*, *3*(1). Retrieved from www.ijresm.com

Shen, J., & Feng, Y. (2023). Recent advances in encapsulation materials for light emitting diodes: a review. *Silicon*, *15*(5), 2163–2172. https://doi.org/10.1007/s12633-022-02171-y

Sun, Z., Li, J., Yu, M., Kathaperumal, M., & Wong, C.-P. (2022). A review of the thermal conductivity of silver-epoxy nanocomposites as encapsulation material for packaging applications. *Chemical Engineering Journal*, *446*, 137319. https://doi.org/10.1016/j.cej.2022.137319

Tavakolibasti, M., Meszmer, P., Kettelgerdes, M., Bottger, G., Elger, G., Erdogan, H., … Wunderle, B. (2022). Structural-thermal-optical-performance (STOP) analysis of a lens stack for realization of a digital twin of an automotive LiDAR. *2022 23rd International*

Conference on Thermal, Mechanical and Multi-Physics Simulation and Experiments in Microelectronics and Microsystems (EuroSimE), 1–7. IEEE. https://doi.org/10.1109/EuroSimE54907.2022.9758897

Thaine. (2020). LED strip anatomy explained. Retrieved from Littleanvil.com website: https://littleanvil.com/journal/2020/4/16/led-strip-anatomy-explained

Vairavan, R., Sauli, Z., & Retnasamy, V. (2013). High power LED heat dissipation analysis using cylindrical Al based slug using Ansys. *RSM 2013 IEEE Regional Symposium on Micro and Nanoelectronics*, 186–189. IEEE. https://doi.org/10.1109/RSM.2013.6706504

Vairavan, R., Sauli, Z., Retnasamy, V., Ismail, R. C., Nor, M., Nadzri, N. S., & Kamarudin, H. (2013). High power LED thermal and stress simulation on copper slug. *2013 UKSim 15th International Conference on Computer Modelling and Simulation*, 294–298. IEEE. https://doi.org/10.1109/UKSim.2013.150

Xu, Z., Wang, T., & Che, Z. (2020). Droplet deformation and breakup in shear flow of air. *Physics of Fluids*, *32*(5). https://doi.org/10.1063/5.0006236

Zhang, R., Ricky, W., & Lo, J. C. C. (2015). Lens forming by stack dispensing for LED wafer level packaging. *IEEE Transactions on Components, Packaging and Manufacturing Technology*, *5*(1), 15–20. https://doi.org/10.1109/TCPMT.2014.2348320

Zhao, Z., & Ye, J. (2013). Design key points for high power LED encapsulation. *Advanced Materials Research*, *651*, 705–709. https://doi.org/10.4028/www.scientific.net/AMR.651.706

APPENDIX A

Table A.1: Dispenser height and point values

Height(mm)	Point Values (epoxy VOF)	
	A	B
4.0	0.317	0.373
6.0	0.324	0.407
8.0	0.305	0.417
10.0	0.293	0.425
12.0	0.281	0.435

Table A.2: Dispenser height, time steps and time taken

Height (mm)	Time steps	Time taken (s)
4.0	1000	0.01
6.0	1100	0.011
8.0	1500	0.015
10.0	1900	0.019
12.0	2300	0.023

Table A.3: Dispenser velocity and point values

Velocity (m/s)	Point Values (epoxy VOF)	
	A	B
0.3	0.083	0.096
0.4	0.174	0.206
0.5	0.308	0.383
0.6	0.402	0.409
0.7	0.463	0.451

Table A.4: Dispenser velocity, time steps, and time taken

Velocity (m/s)	Time steps	Time taken (s)
0.3	2700	0.027
0.4	2000	0.02
0.5	1500	0.015
0.6	1250	0.0125
0.7	1100	0.011

Table A.5: Dispenser offset and point values

Offset (mm)	Point Values (VOF epoxy)	
	A	B
0.10	0.544	0.122
0.15	0.851	0.082
0.20	0.856	0.032
0.25	0.868	0.015
0.30	0.873	0.007

Table A.6: Dispenser offset, time steps, and time taken

Offset (mm)	Time steps	Time taken (s)
0.10	1500	0.015
0.15	1700	0.017
0.20	2000	0.020
0.25	2300	0.023
0.30	2600	0.026